Deflection and collapse of steel-supported beams and floors during fire test

Harmathy, T. Z.

Publisher's version / Version de l'éditeur:
https://doi.org/10.4224/20338260
Internal Report (National Research Council of Canada. Division of Building Research), 1960-08-01

NATIONAL RESEARCH COUNCIL
CANADA
DIVISION OF BUILDING RESEARCH

DEFLECTION AND COLLAPSE OF STEEL-SUPPORTED BEAMS AND FLOORS DURING FIRE TEST

by
T. Z. Harmathy

Internal Report No. 203
of the
Division of Building Research

OTTAWA
August 1960

PREFACE

The rating of beams and floors as to fire resistance must at present be based on the results of a large-scale test carried out in a furnace designed for the purpose. Such tests are expensive and this restricts the number that can be carried out to a relatively small proportion of the possible constructions for which rating information may eventually be required. A search for a less costly basis for prediction of fire resistance and for ways of extending the usefulness of such large-scale tests as can be carried out is therefore justified.

Some of the major factors involved in fire resistance of floors and beams are now being investigated. As a first step attention has been directed to an examination of the time-temperature effects on the strength and deflection of the steel components of floors and beams and to the relationship between these and deflection and collapse during fire test. The first results from this study are now reported. The author, a mechanical engineer and a research officer with the Fire Research Section, is in charge of studies on fire resistance of building components.

Ottawa
August 1960

N. B. Hutcheon
Assistant Director

DEFLECTION AND COLLAPSE OF STEEL-SUPPORTED BEAMS AND FLOORS DURING FIRE TEST

by

T. Z. Harmathy

ABSTRACT

A study on the behaviour of carbon steels at elevated temperatures yields the basis for a method by which the deflection and point of collapse of beams and floors can be calculated if the temperature history of the steel parts is known. The Robertson-Ryan criteria and the 1000°F criterion of ASTM E119 are examined.

Although the standard method for fire tests (ASTM E119) does not require the recording of the deflection of beams and floors during a test, most of the testing authorities think that deflection measurements are valuable additions to those prescribed by the standard. The reason for this concept is probably twofold. Firstly, deflection is a very sensitive indication of a variety of phenomena that take place inside the test specimen, and thus it may yield information that cannot be obtained from standard measurements or from visual observation. Secondly, a steady increase in the rate of deflection is an almost unmistakable sign of the fire test having entered its final stage. Thus from deflection measurements the imminence of collapse can be estimated and, if heavy damages to the furnace are expected, the test can be terminated prior to but reasonably close to the collapse.

In this paper the process of deflection of steel-supported constructions will be analyzed. For such an analysis the temperature history of the steel parts during the fire test must be known. In many cases this can be obtained relatively easily from an analysis of the heat flow through the specimen, by means of some numerical method described in the literature. [See, e.g., (1) or (2). The application of Dusinberre's method for the calculation of fire endurance times will be illustrated in a subsequent publication of the author (3).] In other cases the temperature history of the steel parts is not readily calculable owing to the possible disintegration of some layers of the construction during the test. Although in such cases the variation of the deflection or the time of collapse cannot be predicted, this study may serve as a guide on the interpretation of the deflection measurements.

In the last section of the paper, "Failure Criteria", some theoretical support will be provided for the load failure criteria of Robertson and Ryan (4). Other possible criteria will also be discussed.

Properties of Steel at Elevated Temperatures

It is conventional to separate the strain caused by a certain tensile load in a material into an instantaneous part and a time-dependent part, the latter being termed creep. It is also customary to talk about recoverable and permanent strains, so that one who wants to satisfy both ways of classification has to express the total load strain as consisting of four terms: *

---

* see the end of report for nomenclature.

$$\epsilon_\sigma = \epsilon_{ir} + \epsilon_{ip} + \epsilon_{tr} + \epsilon_{tp} \tag{1}$$

It will be seen, however, that splitting up the load strain into these four terms is not entirely unobjectionable on strictly logical grounds. Especially the separation of the "instantaneous" and "time-dependent" deformations is rather arbitrary. This practice merely reflects the fact that for a long time two basically different test methods have been used for obtaining information on the straining of materials: (i) the ordinary short-time tensile test which is supposed to establish the relationship between ϵ_i, σ and T, viz. the function,

$$f_1 (\epsilon_i, \sigma, T) = 0 \tag{2}$$

and (ii) the creep test, yielding a correlation of the form

$$f_2 (\epsilon_t, \sigma, T, t) = 0. \tag{3}$$

The dependence of the tensile test results on the rate of straining clearly shows, however, that the existence of a strain independent of time, especially in the field of plastic deformation and at higher temperatures, is merely a fiction. From the practical point of view this assumption is, nevertheless, very useful.

Figure 1 shows how the various strains contribute to the deformation of the specimen under a certain constant load (higher than that corresponding to the yield point), and how the deformation diminishes after the removal of the load.

Neglecting the inertia of the mass, ϵ_{ir} is really an instantaneous response to the stressing. It is the familiar elastic strain.

The other recoverable strain, ϵ_{tr}, is called "anelastic strain" and like ϵ_{ir} increases linearly with the load (for a given time). A remarkable feature of the anelastic strain is that after a high initial variation it levels off within a period relatively short compared with the time of fracture, although it is not quite clear whether it approaches a limiting value (5) or continues growing indefinitely (6). Because of its rapid initial increase ϵ_{tr} generally constitutes a large portion of the transient (primary) creep.

The variation of the elastic strain with the temperature is well known. Figure 2 shows the temperature dependence of the modulus of elasticity and represents an average of measurements reported in the literature (7, 8, 9). From Fig. 2 it can be seen that with constant load the elastic strain increases with rising temperature.

The effect of temperature on the anelastic strain has not yet been studied. However, knowing the behaviour of metals at room temperature one can conclude with certainty that as the temperature is reduced the "levelling-off" period decreases sharply and thus at sufficiently low temperature the anelastic strain becomes indistinguishable from the elastic strain.

The term "plastic strain" is used for both "instantaneous" and time-dependent nonrecoverable deformations. In this paper, however, only the first rapidly developing portion of the permanent strain will be so called, the portion that is practically absent if the load is below the yield point. At lower temperatures this is essentially the only permanent deformation, because the ϵ_p vs t curve levels off rather abruptly into a very nearly horizontal section (10). For steel at room temperature the speed of this "instantaneous" deformation seems to be of the order of

0.1 in./in./sec, therefore tensile tests performed at any lower speed yield roughly identical results (11).

At higher temperatures the rapidly developed plastic strain is followed by a slowly increasing deformation. This latter strain will only be regarded here as the "time-dependent" permanent strain, ϵ_{tp}, and will be called "plastic creep". There is, of course, a gradual transition between the regions of ϵ_{ip} and ϵ_{tp}, therefore, as already mentioned, their separation is somewhat artificial. It is conventional to take the permanent strains correlated with the load stresses by the curve of an ordinary short-time tensile test at the given temperature as the "instantaneous" plastic deformations. Since the speed of such tests is of the order of 10^{-3} in./in./sec and the resulting deformation is of the order of 0.01 in./in., it may be said that the plastic strain is a short-time response to the stressing, and develops in a time of the order of 10 sec. Plastic creep, on the other hand, is a deformation progressing at a fairly constant but much lower rate.

During a fire test the temperature of the steel parts varies continuously; the load may also be variable, as will be seen in a subsequent section. From the foregoing it is plain that there will be a strain response to these variations which is practically instantaneous at lower temperatures and strongly time-dependent at higher temperatures. Again, some explanation is needed of what is meant by "lower" and "higher" temperatures. Based on the test results of Kerkhof and Clark (12) it seems reasonable to assume that in the case of carbon steels up to about 600°F the creep following a quasi-instantaneous strain response is negligible, in other words, the deformation can be predicted from the stress-strain curves obtained by ordinary short-time tensile tests alone. It is around 750°F that creep becomes increasingly significant. Above 750°F therefore, knowledge of the creep characteristics of steel is also needed for the prediction.

A considerable amount of information is available from the literature regarding the short-time properties of carbon steels at elevated temperatures. Figure 3 shows the appearance of the $\sigma = \sigma(\epsilon_i, T)$ surface for a typical structural steel. The shape of the surface is nearly the same for any hot-rolled carbon steel of ferrite-pearlite structure, although the actual values may differ significantly.

It is seen from Fig. 3 that slightly below 600°F the yield point completely disappears. At higher temperatures there is no real elastic limit and elastic and plastic strains occur simultaneously even at moderate stresses. (This fact explains why the yield strength had to be defined as the stress at which a specified nonrecoverable deformation, generally 0.2 per cent, is attained.)

The two most important pieces of information that one can obtain from Fig. 3 are the variation of the ultimate and the yield strengths with the temperature. A separate plot of these two functions is shown in Figure 4. Data from a number of sources (8, 11, 13 to 18) have been used to draw the "best curves". Since for steels of different composition the loss or gain in strength at elevated temperatures is roughly proportional to the strength at room temperature (13), it was possible to use the dimensionless variables σ_U/σ_{UR} and σ_Y/σ_{UR} instead of σ_U and σ_Y, and thus extend the usefulness of the plot.

The curves are applicable to most of the hypo-eutectoid carbon steels, namely to the low- and medium-carbon hot-rolled or cast steels in "as rolled", "as cast" or annealed condition. (These conditions may be referred to as "standard conditions".) Rigorously, they cannot be used in the case of cold-worked steels due to the much higher σ_{YR}/σ_{UR} ratio,

and in the case of quenched and tempered steels, because of the more rapid loss of strength with increasing temperature. However, since after a prolonged heating at higher temperatures the distortion of the microstructure caused by the cold work tends to relieve, and the martensite formed by quenching transforms into a pearlite-like sorbite structure, it is reasonable to assume that above 750°F the curves of Figure 4 are applicable to any hypo-eutectoid carbon steel, irrespective of the heat treatment and the mechanical work performed on them, if for σ_{UR} and σ_{YR} the values corresponding to the standard conditions are used.

The accuracy of these curves is probably not better than ± 20 per cent. If higher accuracy is required, similar σ_U vs T and σ_Y vs T plots for the specific steel must be obtained.

The usefulness of such plots can further be extended by the inclusion of ϵ_{ip} = constant curves. Figure 4 shows a number of such curves. (By definition the curve of the yield strength is also an ϵ_{ip} = constant curve.) Because of the meagreness of the available information in this field the accuracy of these curves is thought to be poorer than ± 20 per cent.

In contrast to the rather wide applicability of the σ_U/σ_{UR} and σ_Y/σ_{UR} curves of Figure 4, at present little generalization is possible in correlating the creep characteristics of different carbon steels. Creep is an extremely structure-sensitive property, therefore such factors as composition, cold work, heat treatment, grain size, and melting practice may significantly influence its development.

Temperature is the only variable whose effect on creep is fairly well established. Several attempts have therefore been made to formally eliminate T from correlation (3) by combining it with another

variable, either the time (19 to 22), or the creep rate (23, 24) in the range of "secondary creep" where $d\epsilon_t/dt$ is nearly constant. Although the theoretical support behind these combined variables is not always convincing, if used with proper limitations they may be useful in simplifying the graphical representation and extrapolation of the test data.

In Figure 5 the creep strain (ϵ_t) of an annealed carbon steel of about 0.4 per cent carbon is plotted against the "temperature compensated time" (Θ) of Dorn (19, 20) for several σ = constant values. In spite of the criticism of Garofalo, Smith and Royle (25), and the fact that Dorn himself did not recommend the use of this combined variable, Θ, for correlating data below one half of the melting temperature of the metal (in this case about 1050°F), it was found that the curves of the graph are capable of satisfying a number of experimental data reported in the Creep Data Book (26), in the whole temperature range where the creep of steel is not negligible (above 750°F), and do not contradict the data reported elsewhere (15, 17, 18, 27). It should be noted, however, that curves in Fig. 5 cannot be regarded as "characteristic" even of carbon steels of similar carbon content. Steels of slightly different microstructure (grain size and shape) may exhibit significantly different creep properties under identical circumstances.

For carbon steels the anelastic creep is probably not very significant (28), thus ϵ_t in the graph is approximately identical with the plastic creep, ϵ_{tp}.

The main reason for using Dorn's temperature compensated time as one of the variables of Fig. 5 is that this choice offers a convenient way of calculating the creep in cases when the temperature is a function

of time. If the definition of Θ is generalized in the following way:

$$\Theta = \int_0^t e^{-\frac{\Delta H}{RT_a}} dt \qquad (4)$$

the creep can be determined as a function of time from the ϵ_t vs Θ plot, after obtaining values of Θ by graphical integration of the exp $(-\Delta H/RT_a)$ vs t curve. (This procedure will be shown in the following section.)

Note that for ΔH the value recommended by Dorn for pure iron has been used. With that, $\Delta H/R \approx 70,000°R$.

Figure 6 is a replot of Fig. 5, and is a condensed representation of the information obtainable from Figs. 7, 8 and 9. The fair agreement between the values yielded by these graphs and those reported in the literature (15, 16, 17, 27) also confirms the validity of the plot in Fig. 5.

In Fig. 7 the fracture in 15 sec curve is also shown to demonstrate an interesting linkage between the short-time and the creep properties of the material. According to a previous statement the "instantaneous" plastic strain is that part of the plastic deformation which develops in a time of the order of 10 sec. The creep developing in 15 sec (even up to the point of fracture) is therefore no more a creep, but rather a quasi-instantaneous response to the stressing. In this light the agreement between the 15-sec creep fracture strength and the ultimate strength obtained from short-time tensile tests for the same material is not surprising.

Very little information is available on the behaviour of steel under compression at high temperatures. It seems reasonable to assume, however, that the existance of the remarkable symmetry in the behaviour of metals under tension and compression is independent of the temperature, therefore the above correlations and statements, in general, hold true for

the case of compressive load as well, supposing the deformation caused by the load is not very significant (say, if $\epsilon_\sigma < 0.01$).

So far the strains connected with the loading of the material have been discussed. There is one more kind of strain, additive to the load strain but practically independent of the load; the strain caused by thermal expansion of the steel. The thermal strain is an "instantaneous" response to the temperature variation, and is completely recoverable.

The information given in (29) has been used to plot α, the mean coefficient of thermal expansion of steel between 32°F and T, against T in Fig. 2. Data reported elsewhere (17, 30, 31) are in good agreement with those plotted in the figure.

With the aid of the α vs T correlation the thermal strain is obtained as

$$\epsilon_T = {}_T\alpha\,(T - 32) - {}_{T_o}\alpha\,(T_o - 32) \qquad (5)$$

where ${}_T\alpha$ and ${}_{T_o}\alpha$ are values of α pertaining to temperatures T and T_o, respectively.

Deflection and Collapse of the Fire Test Specimen

Having studied the properties of carbon steels at elevated temperatures, an attempt can now be made to predict the behaviour of steel-supported specimens during a fire test. Examples will be used to illustrate the general scheme of the calculations involved, and to point out the immediate cause of the collapse.

The accuracy of such calculations is limited by the following factors:

(a) Since data on the properties of the specific steel employed in the

construction are not readily available, one must base the calculations on the information presented in a more or less generalized form in the previous section.

(b) Even in a steel-supported structure the steel is not the only load-bearing material. Consequently the load carried by the steel parts is somewhat indefinite and, as a rule, varies throughout the test.

(c) Owing to spalling or disintegration of the protection the variation and distribution of the temperature in the steel structure may not follow a simple rule.

(d) If members loaded with bending moment occur in the structure, the calculation of the plastic deformation becomes very tedious, and often simplifying assumptions are needed.

The following example has been chosen in such a way as to eliminate the last three difficulties. The deflection of a steel truss will be examined. The truss is protected by asbestos sprayed on expanded metal lath, as shown in Fig. 10a. Since the load-bearing capacity of the protection is obviously negligible, the stress in the members of the truss is calculable from the imposed load and can be taken as constant throughout the test. The stress distribution in the structure is shown in Fig. 10b. As is customary, the + sign is used for tensile stresses. There are no members in the structure loaded with bending moment.

The truss is said to have been built from hot-rolled structural steel sections of 72,000 lb/in.^{2} tensile strength.

The temperature of the lower chord, the web members, and the upper chord is assumed to vary in the way shown in Fig. 11a.

The first step is to calculate the strain of each individual member as a function of time. *

The thermal and elastic strains can be calculated by means of Fig. 2. The procedure is quite straightforward; only the result is shown here (see Figs. 11b and 11c).

Figure 4 can conveniently be used for determining the variation of the plastic strain. Since the load is constant during the test, each member of the truss can be represented in the figure by a σ/σ_{UR} = constant horizontal line. For example, member 12 is represented by the $\sigma/\sigma_{UR} = 19,840/72,000 = 0.276$ line (shown as a dashed line). This line intersects the $\epsilon_{ip} = 0.002$, 0.01 and 0.02 curves at 1090°F, 1190°F, and 1223°F, respectively. By finding the times at which these temperatures are reached (from Fig. 11a) three points of the ϵ_{ip} vs t curve of member 12 are gained. This curve, together with those obtained for other members in a similar way, is shown in Fig. 11d.

For determining the ϵ_t vs t correlations first the $\exp(-70,000/T_a)$ vs t curves should be plotted. This has been done in Fig. 11e, on the basis of the information supplied by Fig. 11a. The Θ vs t curves (Fig. 11f) are then obtained by graphical integration [see Eq. (4)]. Finally from Fig. 5 the variation of the ϵ_t's are determined by reading the corresponding $\epsilon_t - \Theta$ values along the σ = constant curves representing the various members of the truss (see Fig. 11g).

---

* After performing a few similar calculations the reader will see that in certain members certain strains are ineffective, others unimportant from the point of view of the truss deflection, thus the calculations may be simplified considerably.

Once the strain of each member is known, the deflection at any point of the truss is obtained by means of Eq. (24) of Appendix A. In order to calculate the central deflection, a Maxwell diagram has to be constructed with a (real or fictitious) P force located above the central joint of the truss. The graphical procedure is shown in Fig. 10c where the values of dS_{Pm}/dP are also listed.

From the additivity of the various strains, as expressed by the equation

$$\epsilon_m = \epsilon_{Tm} + \epsilon_{irm} + \epsilon_{ipm} + \epsilon_{tm} \tag{6}$$

and from Eq. (24) it follows that

$$y = y_T + y_{ir} + y_{ip} + y_t \tag{7}$$

i.e., the truss deflections caused by the various strains are also additive.

The variation of y_{Tc}, y_{irc}, y_{ipc}, and y_{tc} as well as that of the resulting total central deflection, y_c, is plotted against the time in Fig. 11h. It is seen that, excepting a small "bump" caused by thermal expansion effects, the deflection varies very little during the first 2 hours. Then, roughly as the temperature of the lower chord exceeds 1000°F, the deflection develops with increasing rate up to the point where the truss collapses owing to the instability induced by excessive deflection. According to these calculations the collapse is expected to happen around 2 hr 35 min.

The dashed curve in Fig. 11h shows the deflection of the same truss in the case where the temperature of the members varies according to the dashed curves of Fig. 11a. It can be concluded that once the temperature of the lower chord exceeded 1000°F the rate of the further temperature increase has but a moderate effect on the time of collapse.

Figures 11g and 11h show that the immediate cause of the collapse is the creep of member 12. In fact, if the time of collapse is only of interest it can be predicted with a reasonable accuracy from an ϵ_t vs t plot for member 12 alone, thus most of the calculations just described can be omitted.

Each truss contains one (or two equivalent) such "key member" on which the time of fire endurance depends. This key member is generally easily recognizable; it is, as a rule, the central member (or those left and right from the centre) of the lower (stretched) chord, where the highest stresses and temperatures are met. In exceptional cases, however, the collapse may be due to the buckling of some strongly compressed member among the web members or in the upper chord. (In the above example it may be checked whether members 7, 17, 10 and 14 are liable to buckle earlier than 2 hr 35 min.)

It has been mentioned that if there are bending stresses in the steel support, the calculation of the deflection is very tedious. Employing steel sections or girders, loaded with bending moment is, however, a common practice in floor design. This study would not be complete, therefore, without at least showing the steps involved in such calculations.

Figure 12a shows an 8-in. wide flange beam of 31 lb/ft, protected with sprayed asbestos. It is assumed that the temperature of the bottom fibre (T_o) and the top fibre (T_{VIII}) of the beam varies in the same way as that of the lower and upper chords, respectively, of the truss in the previous example (see Fig. 11a), and at the intermediate points Nos. I, II, ... VII (shown in Fig. 13a) the temperature is calculable in the following way:

$$T_I = T_o - \Delta T;\ T_{II} = T_o - 2\Delta T;\ \ldots\ T_{VII} = T_o - 7\Delta T$$

where $\Delta T = (T_o - T_{VIII})/8$. The temperature distribution in the beam at 2 hr 30 min after the beginning of the test is shown in Fig. 13b.

To calculate the deflection, first the stress and strain distribution in the section at different distances from the support should be computed. This involves a rather lengthy trial-and-error method which will be described in a subsequent publication (32). Only the result of such calculations is shown here in Figs. 13c and 13d. The straight lines and curves show the strain and stress distributions, respectively, at the moment when the temperature distribution is as shown in Fig. 13b.

From the slope of the straight lines the radius of curvature of the beam at the given points can be calculated. The variation of the curvature along the length of the beam has been plotted in Fig. 12b. Since

$$\frac{d^2y}{dx^2} = \frac{1}{\rho} \tag{8}$$

the shape of the deformed beam has been obtained by repeated graphical integration of the $1/\rho$ vs x curve, as shown in Figs. 12c and 12d.

In the case of wide flange beams and girders it is very often permissible to neglect the load-bearing capacity of the web. If this simplification is used, the knowledge of the temperature history of the lower flange is enough to predict the approximate variation of the deflection or the point of collapse.

Generally the highest tensile stresses and temperatures occur in the central portion of the lower flange, therefore the deflection and collapse of the beam or girder will largely depend on the creep of this portion alone. The length of this "key portion" is, of course, somewhat

indefinite; it can only be defined rather vaguely as "the portion of the bottom flange where the creep is significant". In spite of its vague meaning the idea of the "key portion" may serve a useful purpose, as will be seen in the next section of this paper.

Although a steadily increasing rate of deflection is characteristic of the final stage of the fire test, a roughly exponential increase, like that shown in Fig. 11h, is fairly exceptional. The reason for this is that a truss or a beam rarely exists alone; they are usually elements of a more complex floor or roof construction. Because of the varying interaction of the elements, caused by the increasing deflection, the constancy of load on the individual components is rarely fulfilled.

Figure 14 is a diagrammatic picture of a common floor construction. From the point of view of their role in transferring the load to some vertical bearing construction (wall or column) the elements of this floor can be divided into three groups. The upper layer may be termed as the "load receiving" element. This layer is supported at short spans, therefore it is generally a light construction. The components of the second layer will be called here "load transmitting" elements. Because they are acting on somewhat larger spans, they usually contain some reinforcing steel. The elements which span the whole distance between two walls or columns will be termed "load supporting" elements. These are either made from steel (trusses, girders, beams, joists), or are heavily reinforced with steel. Since the behaviour of the whole floor depends, to a great extent, on the behaviour of the supporting elements, an analysis on the deflection of the floor can largely be reduced to an analysis of the deflection of these "key elements". Finally the walls or columns to which all the load imposed on the floor is last transferred, will be termed "load bearing" elements.

Figure 15a (which may be called "load flow diagram") shows how, under design conditions, the various elements contribute to transferring the load to the ground.

During a fire test the supporting elements are, as a rule, under the severest temperature conditions, and since they are spanning the largest distances, their deflection may become significant at such a stage when the strength of the transmitting and receiving elements is barely affected by the heat. These elements will, of course, follow the deflection of the supporting elements, but, as a result of their elastic bending,part of the load that has so far been transferred to the supporting elements will be switched directly to the bearing elements. As the deflection develops the load on the supporting elements continuously decreases, therefore the deflection of the floor will proceed at a reduced rate. Figure 15b shows what the "load flow diagram" may look like toward the end of the fire test.

The variation of deflection of the floor can be followed by a stepwise calculation. First a short period should be chosen during which the load on the supporting element can be regarded as constant and equal to the design load (p_o). The calculation is started by finding the central deflection of the supporting element at the end of this period (y_{c1}), by means of the previously described methods (see Fig. 14). Then, with the temperature conditions prevailing at the end of the period, the fictitious elastic deflection of a central portion of the transmitting and receiving layers should be computed at the place of the supporting element, but on the assumption that the supporting element is removed (y_1^*). Finally the X_1

force should be found which is necessary to produce $y_1^* - y_c$ upward deflection of the above two layers. Knowing the corresponding initial $y_{co} - X_o$ values, the uniform load on the supporting element at the end of the period can be calculated as

$$p_1 = p_o \frac{X_1}{X_o} \quad . \tag{9}$$

The duration of a second period should again be chosen so that the variation of p_1 within the interval is insignificant. Toward the final stage of the test the required time-steps may be as short as 2 to 5 min. During the earlier stages much longer steps are allowable.

The method of finding the magnitude of an X force, which produces a given deflection, may be recognized as an application of Maxwell's method, which is described in a number of handbooks [see e.g., (33)].

The following assumptions may significantly reduce the labour of calculations and still yield acceptable results:

a) The "resistance" of the transmitting and receiving layers to deflection is practically constant during the test, i.e.,

$$y_1^* \approx y_2^* \approx \ldots \approx y_o^*$$

b) The correlation between the deflection and the load on the supporting element is linear and can be expressed as follows:

$$\frac{y_c - y_{co}}{y_{cF} - y_{co}} = \frac{p_o - p}{p_o - p_F} \tag{10}$$

Figure 16 shows another type of floor construction which may be termed "construction with parallel supporting elements". In this case the supporting elements are so closely spaced that transmitting elements may not be necessary.

The load imposed on a concrete slab (receiving element) is shared by six joists (supporting elements). A plastered gypsum lath ceiling provides protection for both the supporting and receiving elements.

The special problem that is met here is the uneven disintegration of the ceiling during the fire test. Disintegration is, as a rule, most rapid around the centre of the construction, so that joists Nos. III and IV will be the first to be exposed to higher temperatures and will thus be the first to creep. With the development of their deflection, part of their load switches first to the neighbouring joists, Nos. II and V which, being at lower temperatures, are still capable of carrying somewhat higher load at lower rate of creep. However, as more and more load is transferred to them, their deflection also accelerates. This, on the other hand, will result in a further transfer of the load towards joists Nos. I and VI and towards the walls. In the final stage of the test, joists Nos. II, III, IV and V will carry less, Nos. I and VI probably more than the design load, and a large portion of the load will be transferred from the receiving element directly to the walls.

Again, if the temperature history of the supporting elements, at least at the key members or key portions, is known, the progress of deflection or the point of collapse is calculable. Because of the complexity of the problem finding a convenient mathématical model is inevitable.

All the constructions that have so far been treated here were simply supported at the ends or along the edges. In the case of other edge

conditions the construction is not free to expand horizontally. Owing to the edge restraint additional stresses develop in the supporting element. Since these stresses vary throughout the test, again a stepwise calculation is required. This, however, can be coupled with the above-described stepwise procedure for finding the stress relief due to increasing deflection.

Again short-time intervals should first be chosen. Starting from known values of the central deflection of the supporting element and of the uniform load on the element at $t = t_m$ (the end of the $t_{m-1} < t \leq t_m$ interval), y_{cm} and p_m, respectively, $y_{c(m+1)}$ and p_{m+1} (those at the end of the $t_m < t \leq t_{m+1}$ interval) can be estimated in the following way. *

$y_{c(m+1)}$ is assumed to consist of two terms:

$$y_{c(m+1)} = \bar{y}_{c(m+1)} - \bar{\bar{y}}_{c(m+1)} \tag{11}$$

where $\bar{y}_{c(m+1)}$ is the central deflection which would develop by the end of the $t_m < t \leq t_{m+1}$ interval under constant load ($= p_m$), in the absence of any edge restraint, and $\bar{\bar{y}}_{c(m+1)}$ is the deflection due to thermal expansion at full edge restraint, in the absence of any imposed load. $\bar{y}_{c(m+1)}$ can be calculated in the previously described way, while $\bar{\bar{y}}_{c(m+1)}$ is to be found by means of the graph shown in Figure 17, which has been plotted on the assumption that the deflected shape of the supporting element is sinusoidal. For ϵ_T the average thermal strain (the mean of the strains of the upper and lower chords, or of the upper and lower flanges) at $t = t_{m+1}$ should be taken.

---

* Since the degree of edge restraint is always somewhat indefinite, it is believed that the accuracy of such calculations cannot be increased significantly even by the use of methods more refined than the one shown here.

When calculating p_{m+1} (the load at the end of the $t_m < t \leq t_{m+1}$ interval) the $\bar{\bar{y}}_{c(m+1)} - \bar{\bar{y}}_{cm}$ difference is regarded as a quasi-instantaneous change of deflection caused by some fictitious load, Δp_{m+1}, applied at $t = t_{m+1}$. After finding the magnitude of Δp_{m+1} in the way shown below, p_{m+1} (the constant uniform load in the $t_{m+1} < t \leq t_{m+2}$ interval) is obtained as

$$p_{m+1} \approx (p_m + \Delta p_{m+1}) \frac{X_{m+1}}{X_m} \tag{12}$$

where X_{m+1}/X_m is the correction for the load relief due to a $(y_{c(m+1)} - y_{cm})$ increase of the deflection during the period.

If the stresses in the supporting element do not exceed the yield point at the prevailing temperatures, Δp_{m+1} is given by

$$\Delta p_{m+1} = p_m \left[\frac{y_{c(m+1)}}{\bar{y}_{c(m+1)} - \bar{\bar{y}}_{cm}} - 1 \right]. \tag{13}$$

If in some member of the truss or at some portion of the beam or girder the stress exceeds the yield point, trial and error calculations are required to find Δp_{m+1}. In such cases, however, $\Delta p_{m+1} \approx 0$ is very often a reasonable approximation.

Calculations of this kind showed that at earlier stages of the fire test the stresses caused by the lack of free horizontal expansion may be very much higher than the design stresses, and may even exceed the elastic limit. As the deflection increases and the creep begins, however, these stresses quickly relieve, so that once the creeping region is attained the edge restraint does not decrease, but (because of the better stability of such constructions) probably slightly increases the time of collapse.

Failure Criteria

Since it is the deformation of the key member on which the deflection and collapse of a truss primarily depends, a satisfactory model of the truss is obtained by regarding all members, with the exception of the key member, as perfectly rigid. For example, Fig. 10d shows the model which in many respects is a fair representation of the truss of Fig. 10a.

From the geometry of the model or from Eq. (24) the following equation will result:

$$y_c = \frac{\ell\, \ell_k}{4d}\ \epsilon_k \tag{14}$$

and hence

$$\frac{dy_c}{dt} = \frac{\ell\, \ell_k}{4d}\ \frac{d\epsilon_k}{dt}\ . \tag{15}$$

Similar expressions can be obtained for the deflection and rate of deflection of uniformly loaded beams or girders, supposing the load-bearing capacity of the web is neglected and ℓ_k is taken as the length of the key portion, ϵ_k as the average creep strain of the key portion.

With this latter meaning ℓ_k is some function of the stress distribution along the bottom flange. Since for a definite type of load (e. g. uniform load) the stress distribution is expressible in terms of σ_{max} (at the midspan) and x/ℓ , and since in a well-designed construction σ_{max} equals the allowable stress, thus being approximately constant, it can be said that the ℓ_k/ℓ ratio is roughly the same for any uniformly loaded beam or girder. Therefore, for beams and girders, Eqs. (14) and (15) can be rewritten as:

$$y_c \approx \beta \epsilon_k \frac{\ell^2}{d} \tag{16}$$

and

$$\frac{dy_c}{dt} \approx \beta \frac{d\epsilon_k}{dt} \frac{\ell^2}{d} \quad . \tag{17}$$

Since fractured members are rarely found in collapsed constructions, the cause of the collapse must be, in most cases, the instability induced by an excessive creep strain of the key portion. Although the ϵ_k at which the instability arises is an indeterminate value, owing to the varying degree of the initial stability of various constructions, one can certainly define an $\epsilon_{k\ell}$ limit below which, for any type of construction, collapse is most improbable. If, therefore, $\epsilon_k > \epsilon_{k\ell}$, or

$$y_c > \beta \epsilon_{k\ell} \frac{\ell^2}{d} \tag{18}$$

this simply means that there exists a probability for collapse, but does not mean that collapse is imminent.

It has been pointed out (see Figure 11g) that a steadily increasing creep rate is an almost certain sign of the final deterioration of the structure. If, therefore, the creep rate is higher than a specified $(d\epsilon_k/dt)_\ell$ limit, i.e.,

$$\frac{dy_c}{dt} > \beta \left(\frac{d\epsilon_k}{dt} \right)_\ell \frac{\ell^2}{d} \tag{19}$$

and if (18) is fulfilled, then collapse will occur within a specified time limit.

By substituting 1/800 for $\beta \epsilon_{k\ell}$ in (18) and 1/150 for $\beta (d\epsilon_k/dt)_\ell$ in (19), these two inequalities can be recognized as being identical with the two criteria of Robertson and Ryan (4), which they developed in an empirical way in order to define the "load failure", i.e. the point at which the collapse is reasonably well approached.

Since for trusses ℓ_k is not related to ℓ, the load failure criteria should be expressed in terms of $\ell \ell_k/d$ rather than ℓ^2/d, with ℓ_k denoting the length of the key member.

Although the Robertson-Ryan criteria are very useful for testing authorities in providing means of saving the furnace from damaging collapses of test specimens without reducing the amount of information obtainable from the test, they offer very little help to those who would like to obtain the fire endurance characteristics of the construction by means of calculation. The calculation of the point of "load failure" is obviously not simpler than the calculation of the time of collapse.

One may object that the feasibility of calculations cannot be an important point of view in wording the failure criteria, since calculated fire endurances are not recognized as being equivalent to the test results. Although the present dislike for calculated results is understandable, nobody can seriously believe that fire endurance is the only field where the scientific advance will fail, and that the monopoly of the test results can be prolonged indefinitely.

When wording the failure criteria it should always be remembered that a fire test is not a reproduction of a building fire, therefore the fire endurance is not the time for which the constructions will actually function in fire. The fire endurance is rigorously just a figure that enables one to compare one construction with another from the point of view of its ability to resist building fires. On this basis, of the many possible cirteria that may serve as a basis for such comparisons, obviously the simplest is the best.

An excellent example of how a failure criterion should be worded is the 1000°F criterion of ASTM E119 for protected steel columns and beams. If, however, the load failure of a beam, which is generally the

supporting element of a floor, can be judged on the basis of the 1000°F criterion, the author wonders why the load failure of the whole floor could not be judged on the same basis.

While the attainment of a fixed temperature limit by the steel parts seems a very sound failure criterion, it may be disputed whether 1000°F is really the proper temperature limit. The steel parts of a floor are generally sized on the assumption of 15,000 to 20,000 lb/in.^{2} allowable stress. Figure 7 reveals that under such load a 0.4C steel will function at least 25 min and perhaps as long as $3\frac{3}{4}$ hr at 1100°F without fracture. This might be taken, therefore, as the failing temperature at the key member or key portion of the supporting element. In the case of a construction with parallel supporting elements, when there are several key members (portions) in the floor, the average temperature of the key members (portions) might be allowed to reach the temperature limit. In other members or at other portions much higher temperatures can be tolerated. Figure 9 shows, e.g., that a member loaded with 5000 lb/in.^{2}, can be kept for 1 hr at 1250°F without attaining a plastic deformation larger than 0.1 per cent, and (from Fig. 7) at 1450°F without fracture.

According to a newer concept in building design certain building elements may be required to pass the fire test without unrepairable damage. The temperature attainable by the steel parts of the construction may, therefore, be limited in such a way as to keep the non-recoverable deformation under a specified value. If, e.g., 0.1 per cent is chosen as the maximum allowable permanent strain, according to Fig. 9, 950°F might be taken as a reasonable temperature limit.

Experimental data (34) show, however, that even with 950°F steel temperature noticeable deflections may occur. This is partly due to the presence of non-ferrous materials which may suffer large permanent

deformation at much lower temperatures, partly to some local stresses developing under the effect of edge restraint or unequal thermal expansions in the construction. It seems that to keep the non-recoverable deformations reasonably small, temperatures much higher than 750°F cannot be tolerated at least at the key members or key portions of the supporting element.

There are strong signs (34, 35) that the prestressed concrete beams must be treated in a completely different way. In such constructions cold-drawn steel wires are generally used which, as has been touched upon previously, behave differently from carbon steels in "standard conditions". Microstructural changes are undoubtedly responsible for the fact that at temperatures as low as 400°F the loss of prestress may result in very noticeable permanent deformation of the construction.

APPENDIX A

It will be shown that the validity of the method of calculating truss deflections (sometimes called the "dummy unit-load method", see, e.g., Ref. (36)) is not restricted to elastic deformations, and can be generalized to include cases where both recoverable and non-recoverable strains occur in the truss members.

The strain energy of the truss is given by

$$U = \sum_{m=1}^{n} \int_{\ell_m}^{\ell_m + \Delta \ell_m} S_m \, d\ell_m . \tag{20}$$

According to Castigliano's theorem the deflection at some j^{th} joint is obtained as

$$y_j = \frac{\partial U}{\partial P_j} = \sum_{m=1}^{n} \int_{\ell_m}^{\ell_m + \Delta \ell_m} \frac{\partial S_m}{\partial P_j} \, d\ell_m . \tag{21}$$

Since

$$S_m = \sum_{i=1}^{s} S_{P_i m} \tag{22}$$

where $S_{P_i m}$ is a linear function of P_i alone

$$\frac{\partial S_m}{\partial P_j} \equiv \frac{d S_{P_j m}}{d P_j} , \tag{23}$$

and because of the linearity, $d S_{P_j m}/d P_j$ is a constant.

Consequently, with $\Delta \ell_m = \ell_m \epsilon_m$

$$y_j = \sum_{m=1}^{n} \frac{d S_{p_j m}}{d P_j} \ell_m \epsilon_m . \qquad (24)$$

If the j^{th} joint is not loaded, a fictitious $P_j \longrightarrow 0$ force should be placed on the joint. By similar reasoning, Eq. (24) will again result.

By substituting ϵ_m from Hooke's law one gets the familiar expression for the elastic deformation of trusses.

The values of $d S_{p_j m} / d P_j$ can most conveniently be obtained graphically, by constructing the Maxwell diagram of the truss loaded with the P_j force alone. Such graphical procedure is seen in Fig. 10c.

In the above derivation it has been assumed that the strain energy is independent of the deflection. It is obvious, however, that since the strain energy is a function of the truss shape, it does depend on the deflection. Consequently in the case of large deflections the correct result is obtained only after successive approximations.

NOMENCLATURE

d	distance between the upper and lower chords of a truss; distance between the upper and lower extreme fibres of a beam or girder, in.
E	modulus of elasticity, lb/in.^{2}
f	function
ΔH	activation energy for creep, Btu/lb mole
ℓ	length of a truss member; length of a portion of a beam or girder; without subscript: span, in.
$\Delta\ell$	change of length of a truss member; change of length of a portion of beam or girder, in.
n	number of truss members, dimensionless
p	uniform load, lb/in.
Δp	load increase, lb/in.
P	force, lb
R	gas constant, Btu/lb mole °R
s	number of loaded joints in a truss, dimensionless
S	force in a truss member, lb
t	time, hr
T	temperature, °F
T_a	absolute temperature, °R
U	energy, lb in.
x	variable length along the length of a beam or girder, in.
X	force, lb
y	deflection, in.
z	variable length along the height of a beam or girder, in.

GREEK LETTERS

α	mean coefficient of thermal expansion, °F^{-1}
β	constant, dimensionless
ϵ	strain, dimensionless

ρ radius of curvature, in.

σ load stress, $lb/in.^2$

Θ $= t \exp(-\Delta H/RT_a)$, temperature compensated time, hr

SUBSCRIPTS

c central

F near the collapse

i instantaneous

i = 1, 2, 3, ... (in Appendix A)

j at the j^{th} joint

k of the key member or key portion

ℓ limiting

m = 1, 2, 3, ... designation of time-intervals or truss members

max maximum

o at t = o

p permanent

P, P_i, P_j due to the forces P, P_i, P_j, respectively

r recoverable

R at room temperature

t time-dependent

T due to thermal expansion

U ultimate

Y yield

σ due to stressing

1, 2, ... at the end of the first, second, ... etc. time-interval

BIBLIOGRAPHY

1. Dusinberre, G. M. Numerical Analysis of Heat Flow. 1st ed. New York, McGraw-Hill, 1949.

2. Schuh, H. Differenzenverfahren zum Berechnen von Temperatur-Ausgleichsvorgängen bei eindimensionaler Wärmeströmung in einfachen und zusammengesetzten Körpern. VDI Forschungsheft 459 Beilage zu "Forschung auf dem Gebiete des Ingenieurwesens", Edition B, Vol. 23, 1957.

3. Harmathy, T. Z. A Treatise on the Theory of Fire Endurance Rating. To be published.

4. Robertson, A. F., and J. V. Ryan. Proposed Criteria for Defining Load Failure of Beams, Floors and Roof Constructions During Fire Test. J. Res., Natl. Bureau Stds., C. Engineering and Instrumentation, Vol. 63C, No. 2, 1959, p. 121.

5. Johnson, A. E. The Creep Recovery of a 0.17% Carbon Steel. J. Inst. Mech. Engrs., Vol. 145, 1941, p. 210.

6. Lubahn, J. D. The Role of Anelasticity in Creep, Tension and Relaxation Behaviour. Trans., Am. Soc. Metals, Vol. 45, 1953, p. 787.

7. Versé, G. The Elastic Properties of Steel at High Temperatures. Trans., Am. Soc. Mech. Engrs., Vol. 57, 1935, p. 1.

8. Withey, M. O., and J. Aston. Johnson's Materials of Construction. 8th ed., New York, Wiley, 1953, p. 762-763.

9. Smith, G. V. Metallurgical Effects on High Temperature Properties of Metals. In "High Temperature Properties of Materials", by the Pennsylvania State Univ., 1954, p. 61-77.

10. Lequear, H. A., and J. D. Lubahn. Certain Departures from Plastic Ideality at Small Strains. Trans. Am. Soc., Mech. Engrs., Vol. 79, 1957, p. 97.

11. Manjoine, M. J. Influence of Rate of Strain and Temperature on Yield Stresses of Mild Steel. Trans. Am. Soc. Mech. Engrs., Vol. 66, 1944, p. A211.

12. Finnie, I., and W.R. Heller. Creep of Engineering Materials. New York, McGraw-Hill, 1959, p. 259.

13. Unwin, W.C. The Testing of Materials of Construction. 3rd ed., New York; Longmans, Green, 1910, p. 328.

14. Menzel, C.A. Tests of the Fire Resistance and Thermal Properties of Solid Concrete Slabs and Their Significance. Proc. ASTM., Vol. 43, 1943, p. 1099.

15. Smith, J.V. Properties of Metals at Elevated Temperatures. 1st ed., New York, McGraw-Hill, 1950, p. 90, 223.

16. Miller, R.F. The Strength of Carbon Steels for Elevated-Temperature Applications. Proc. ASTM, Vol. 54, 1954, p. 964.

17. Mantell, C.L. Engineering Materials Handbook. 1st ed., New York, McGraw-Hill, 1958, p. 3-8, 3-19, 3-21, 4-73, 4-75, 4-76.

18. Simmons, W.F. and H.C. Cross. Elevated-Temperature Properties of Carbon Steels. ASTM Special Technical Publication, No. 180, 1955.

19. Proceedings for Short Course. Mechanics of Creep. The Pennsylvania State University, 1954, p. 1.

20. Dorn, J.E. Some Fundamental Experiments on High Temperature Creep. J. Mech. Phys. Solids, Vol. 3, 1954, p. 85.

21. Larson, F.R., and J. Miller. A Time-Temperature Relationship for Rupture and Creep Stresses. Trans. Am. Soc. Mech. Engrs., Vol. 74, 1952, p. 765.

22. Manson, S.S., and A.M. Haferd. A Linear Time-Temperature Relation for Extrapolation of Creep and Stress-Rupture Data. NACA, TN 2890, 1953.

23. Kanter, J.J., and E.A. Sticka. Creep Rates from Tests of Short Duration. Am. Soc. Metals, Vol. 28, 1940, p. 257.

24. MacGregor, C.W., and J. Fischer. A Velocity-Modified Temperature for the Plastic Flow of Metals. J. Appl. Mechs., Vol. 13, 1946, p. A11.

25. Garofalo, F., G. V. Smith, and B. W. Royle. Validity of Time-Compensated Temperature Parameters for Correlating Creep and Creep-Rupture Data. Am. Soc. Mech. Engrs. Paper No. 55-A-164, 1955.

26. Compilation of Available High-Temperature Creep Characteristics of Metals and Alloys. Compiled by Creep Data Section of Joint Research Committee on Effect of Temperature on the Properties of Metals. Published jointly by ASTM and Am. Soc. Mech. Engrs., 1938.

27. Norton, F. H. The Creep of Steel at High Temperatures. 1st ed., New York, McGraw-Hill, 1929.

28. Cross, H. C., and J. G. Lowther. Long-Time Creep Tests of 18 Cr 8 Ni Steel K19 and 0.35 C Steel K20. Trans. Am. Soc. Mech. Engrs., Vol. 59, 1937, p. 441.

29. Perry, J. H. Chemical Engineers' Handbook. 3rd ed., New York, McGraw-Hill, 1950, p. 200.

30. Handbook of Chemistry and Physics. 30th ed., Cleveland, Chemical Rubber Publ. Co., 1946, p. 1747.

31. ASME Boiler and Pressure Vessel Code, Sec. VIII, Unfired Pressure Vessels, 1956, p. 90.

32. Harmathy, T. Z. Deformation by Creep of Beams Subjected to Variable Temperature. To be published.

33. Timoshenko, S. P. History of Strength of Materials, New York, McGraw-Hill, 1953, p. 205.

34. Mourachev, V. I. Méthodes Adoptées en U. R. S. S. pour l'Etude de la Résistance au Feu des Eléments de Construction, et quelques Résultats Obtenus. Paper prepared for distribution to members of Conseil International du Bâtiment, 1958.

35. Bakke, H. A. Fire Resistance of Prestressed Concrete (in Norwegian). Teknisk Ukeblad, Vol. 105, 1958, p. 651.

36. Merritt, F. S. Building Construction Handbook, 1st ed, New York, McGraw-Hill, 1958, p. 3-46.

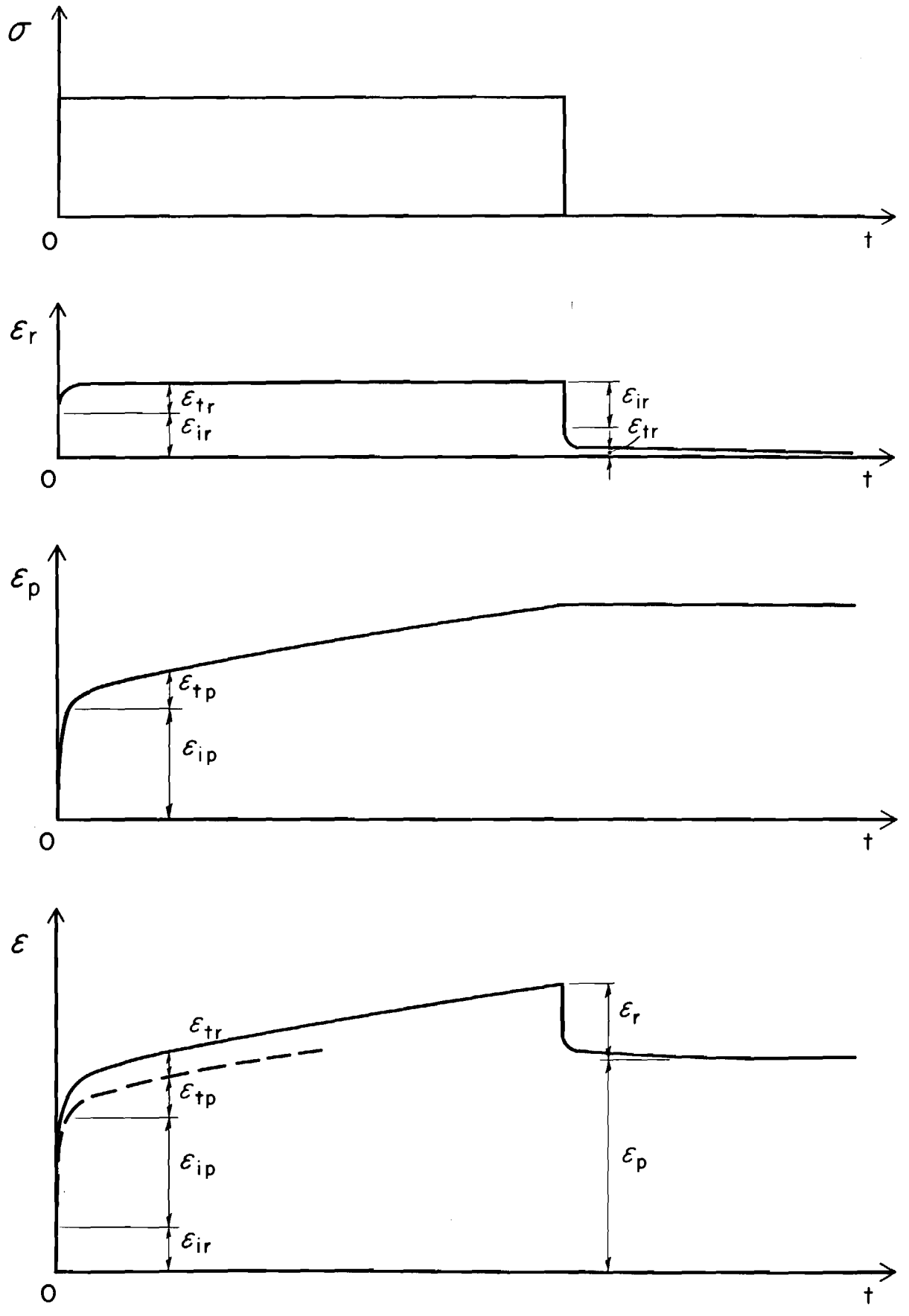

FIGURE 1 STRAINS CAUSED BY LOAD

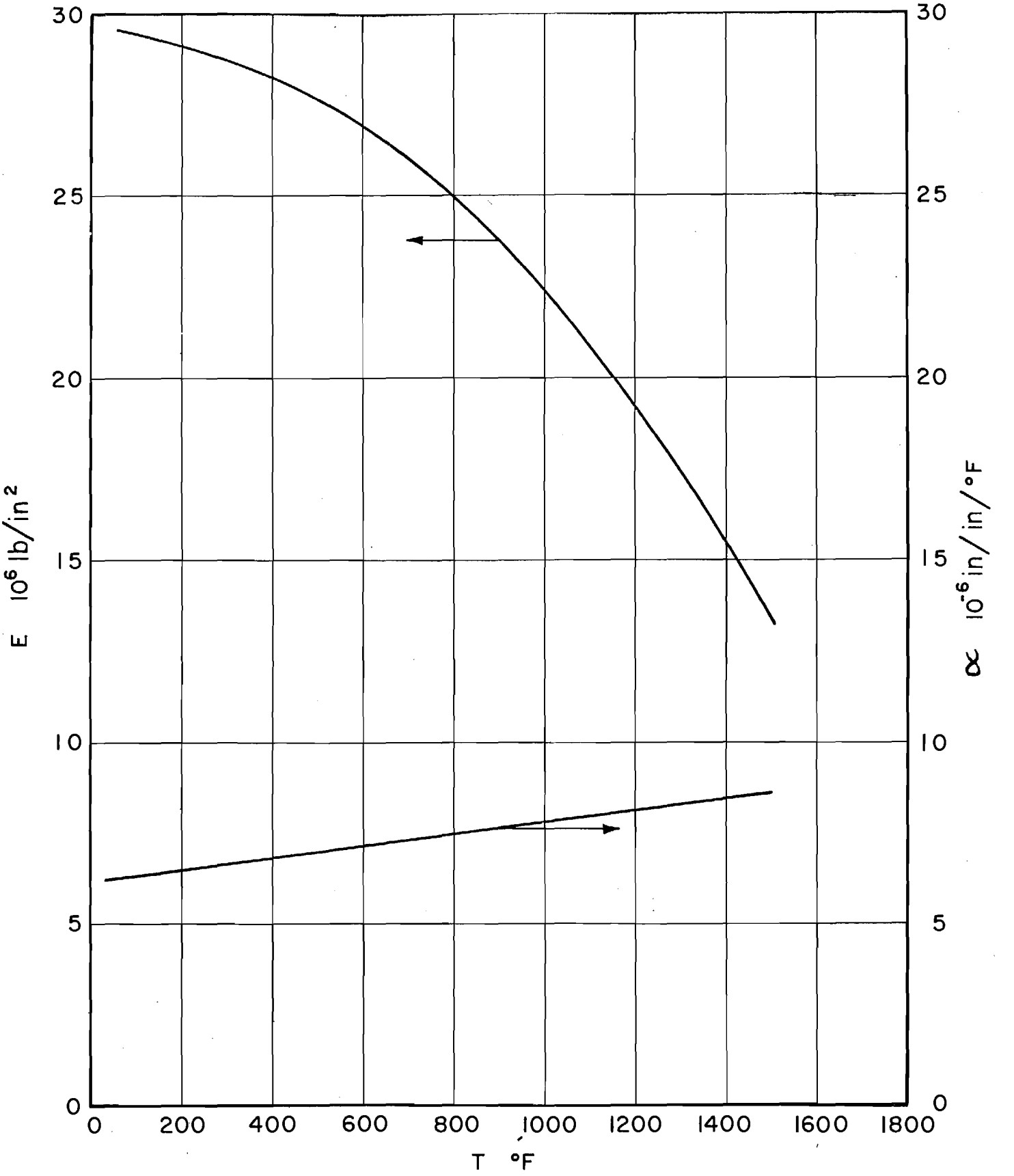

FIGURE 2

MODULUS OF ELASTICITY AND MEAN COEFFICIENT OF THERMAL EXPANSION OF CARBON STEELS

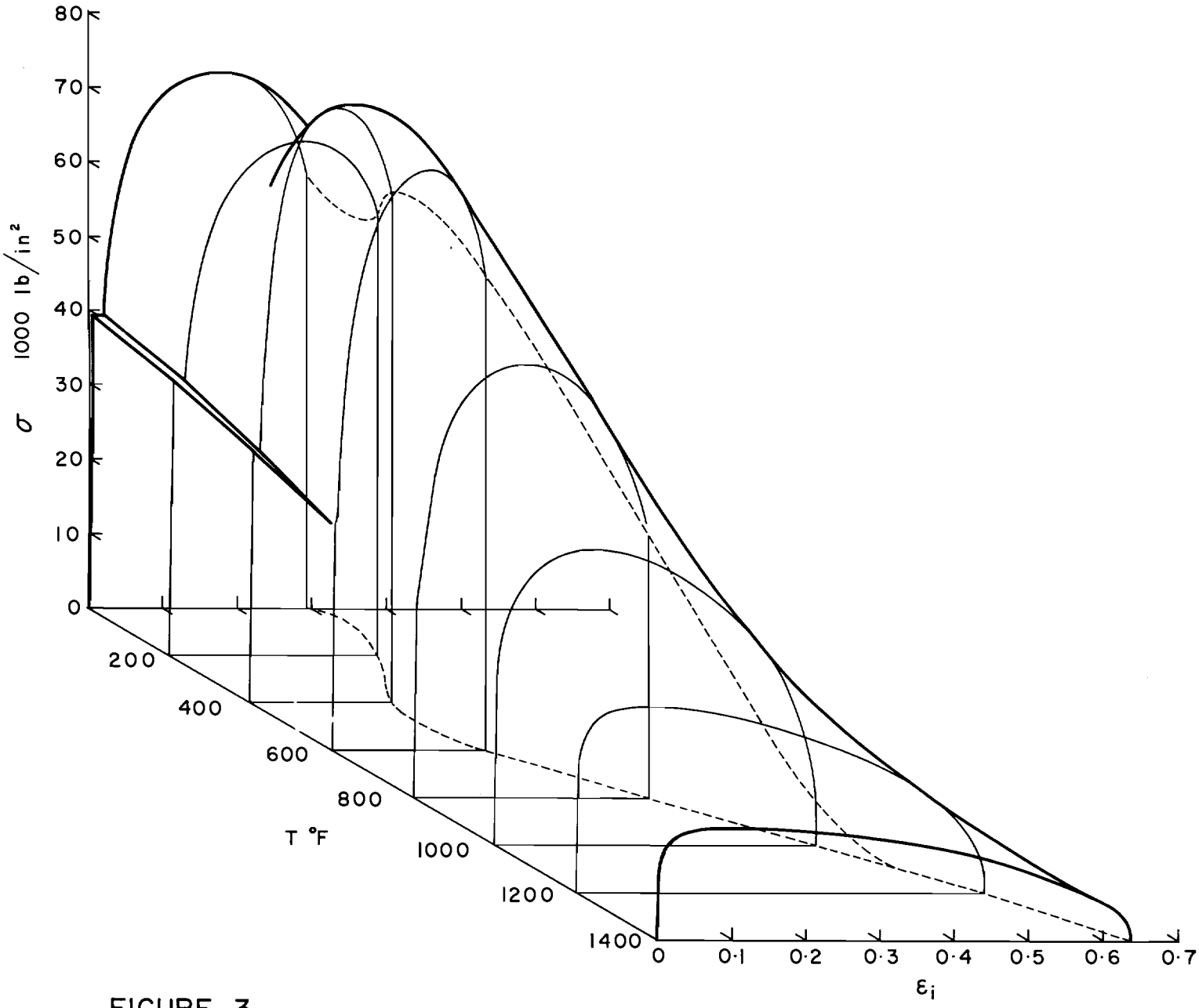

FIGURE 3

THE $\sigma = \sigma(\varepsilon_i, T)$ SURFACE FOR SHORT TIME TENSION TESTS

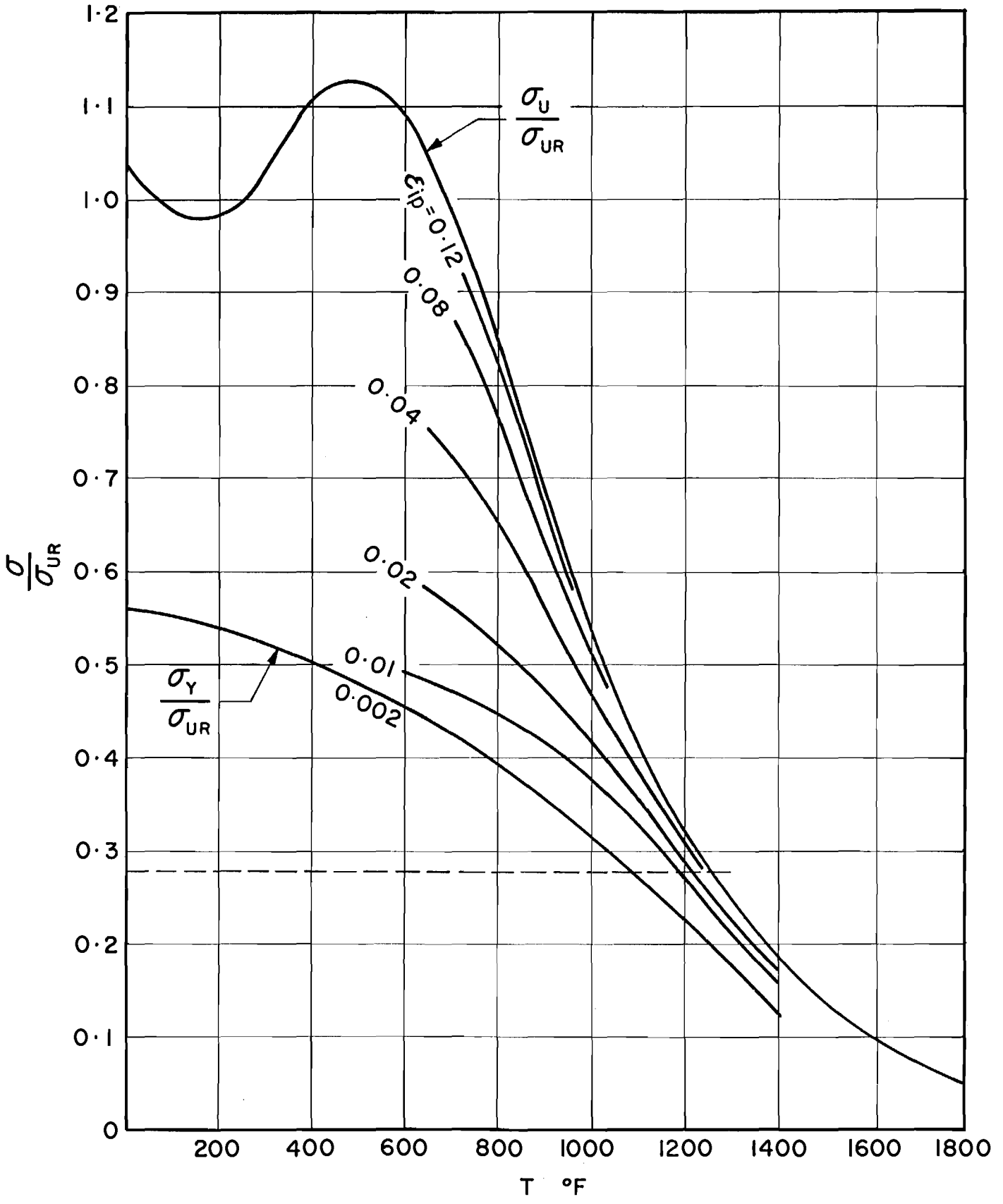

FIGURE 4

GENERALIZED PLOT OF SHORT TIME TENSILE TEST DATA

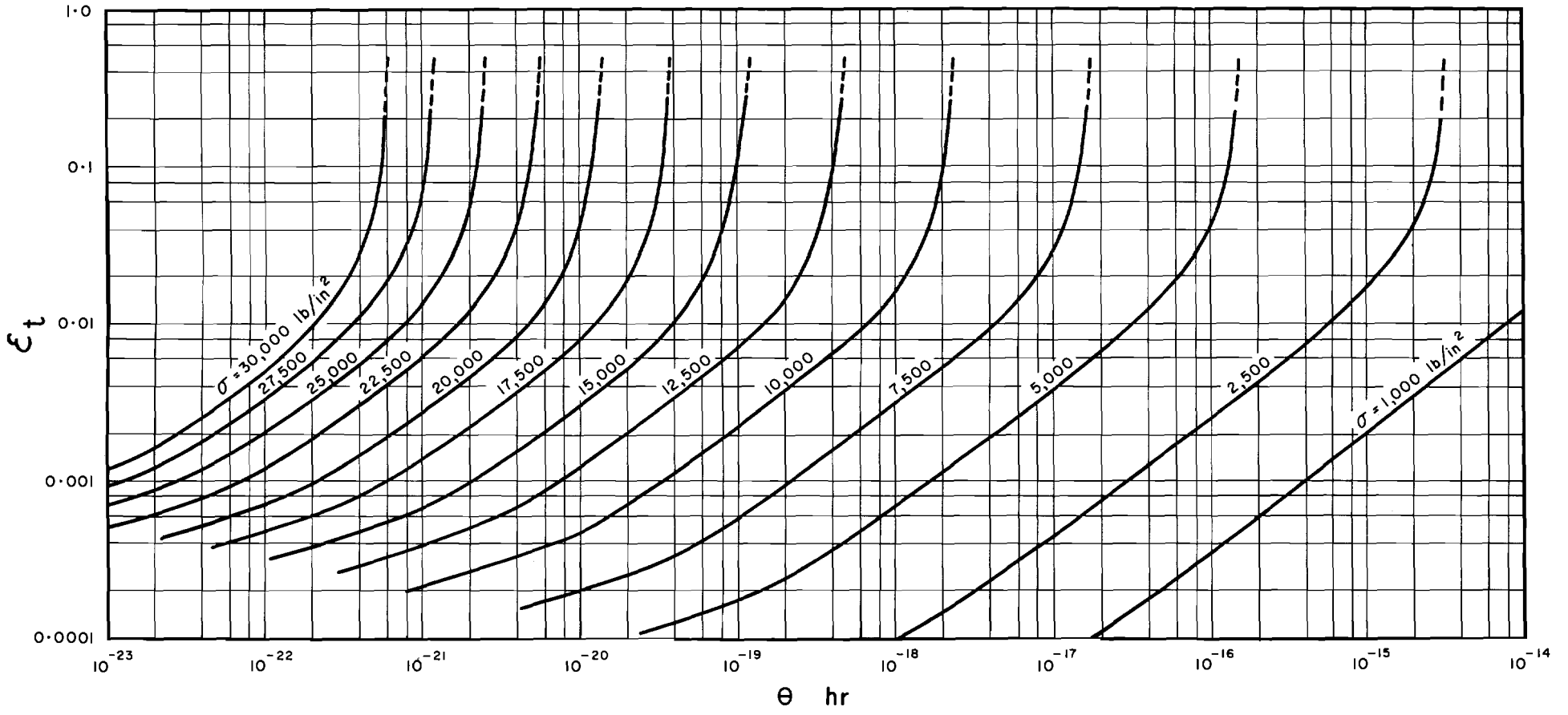

FIGURE 5 CREEP DATA OF A 0·4C STEEL

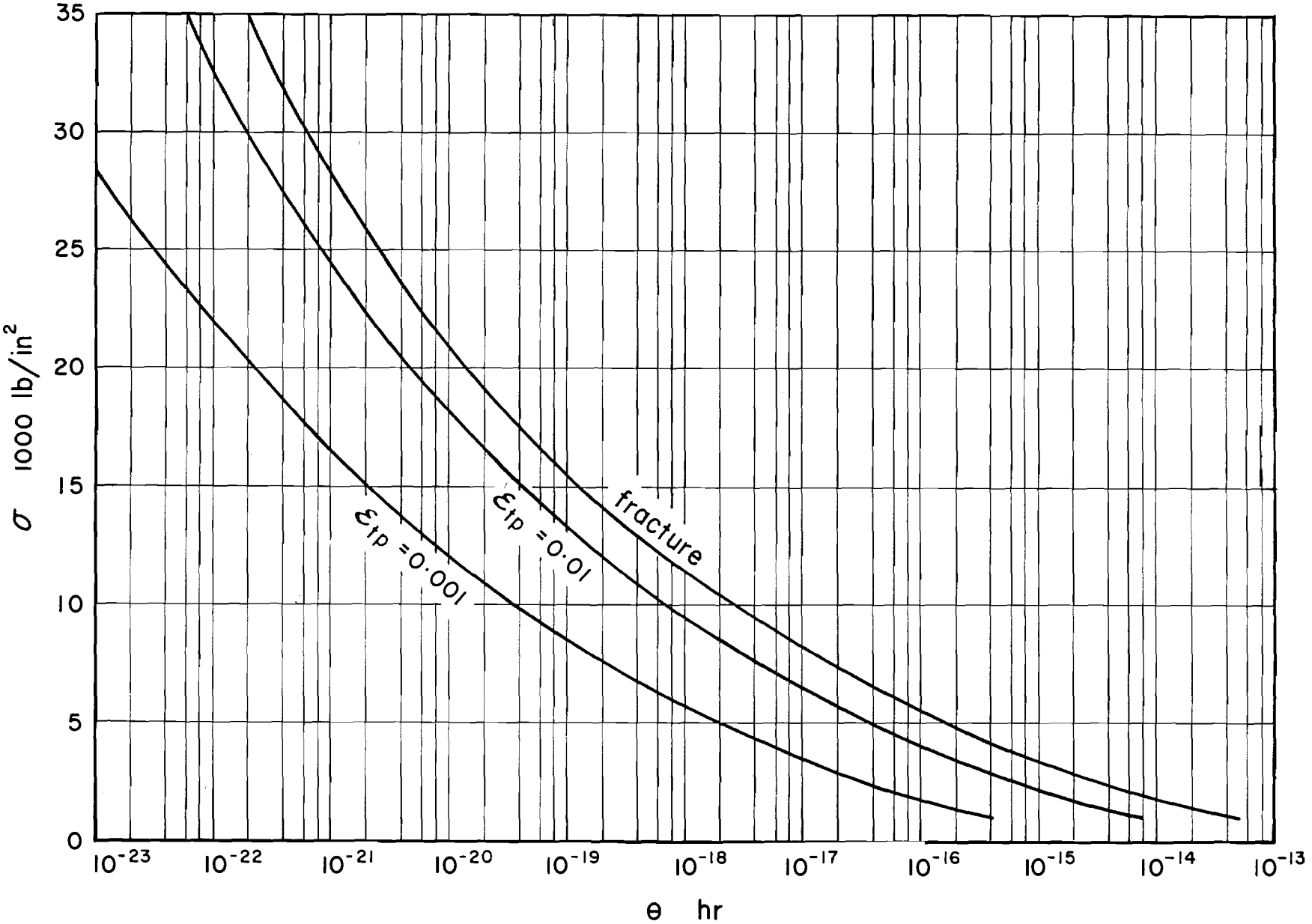

FIGURE 6

CREEP DATA OF A 0·4 C STEEL

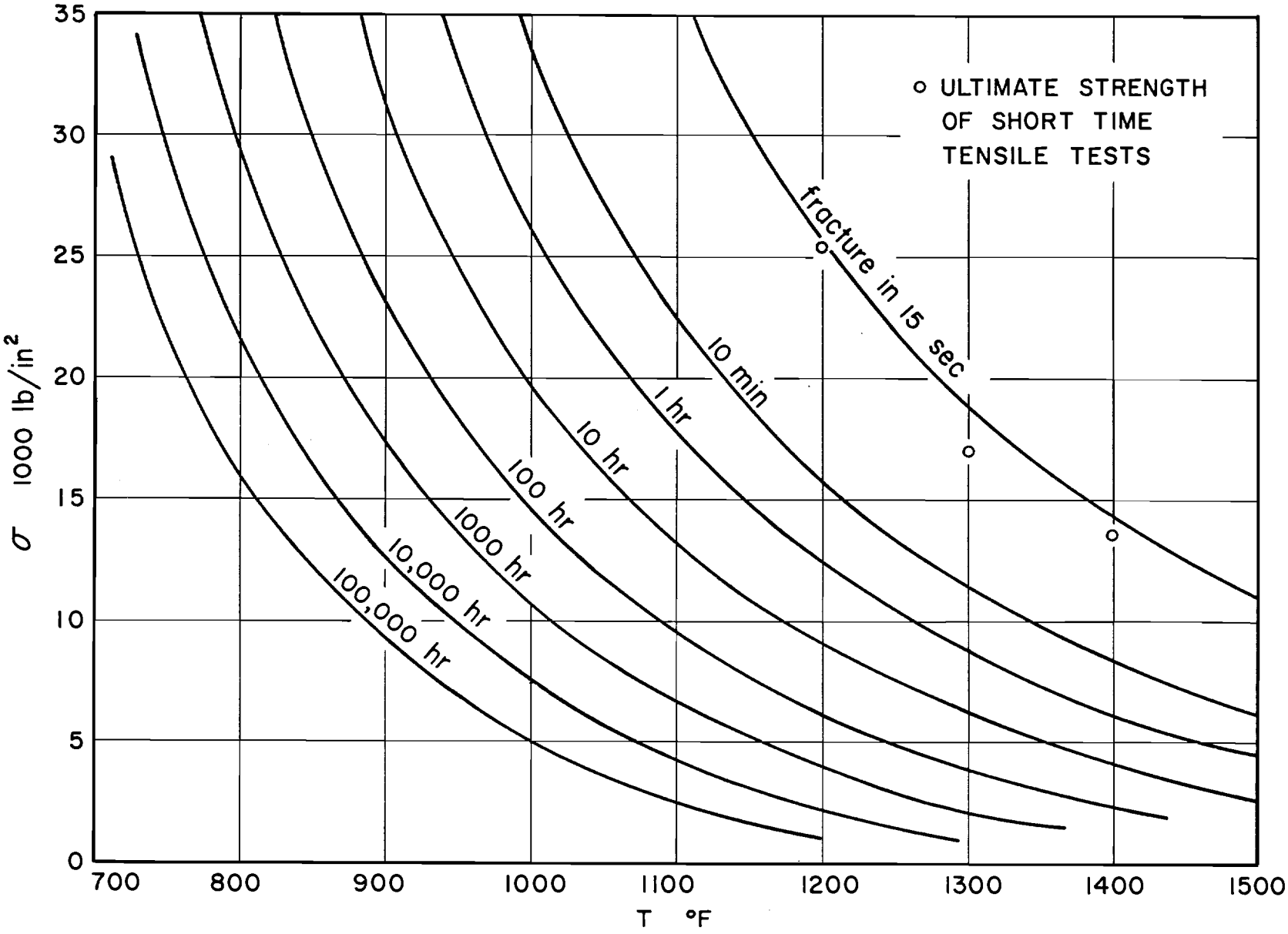

FIGURE 7

FRACTURE BY CREEP OF A 0·4 C STEEL

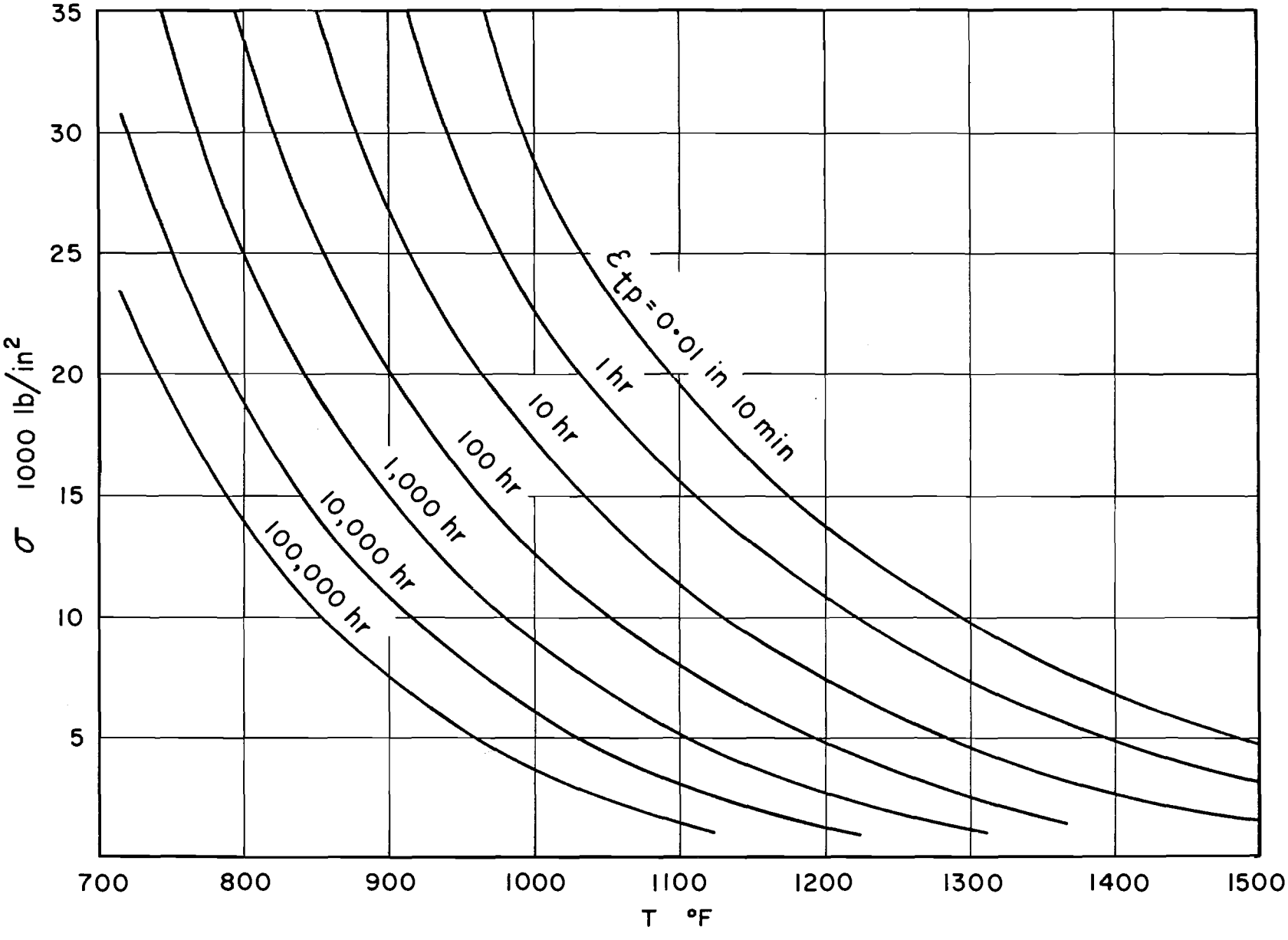

FIGURE 8

1·0% PLASTIC CREEP OF A 0·4C STEEL

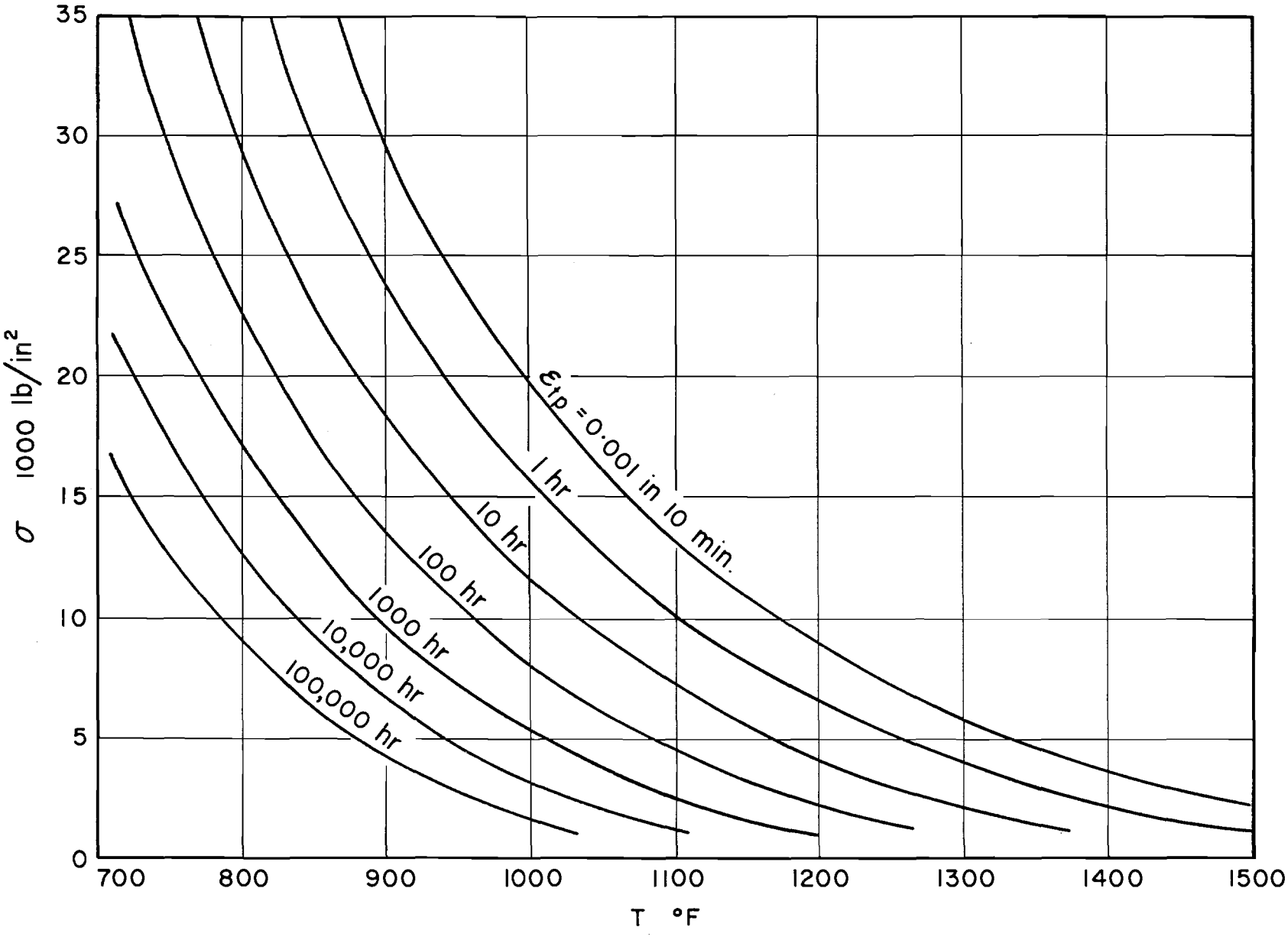

FIGURE 9

0·1% PLASTIC CREEP OF A 0·4C STEEL

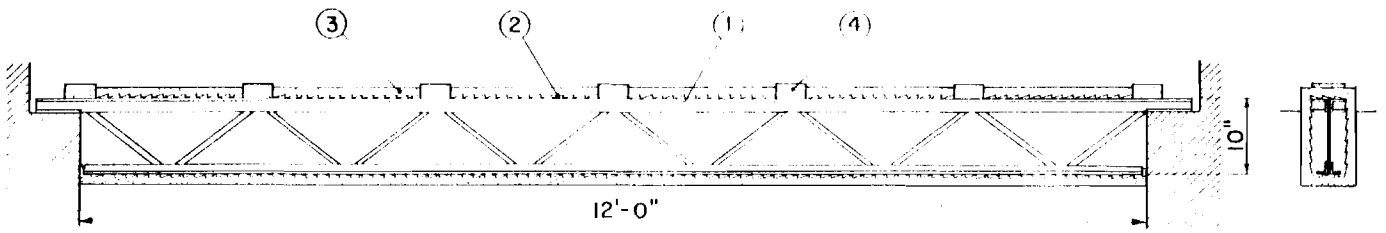

a) Diagrammatic Section of the Truss

① Steel Truss
② Metal Lath
③ Sprayed Asbestos
④ Brick

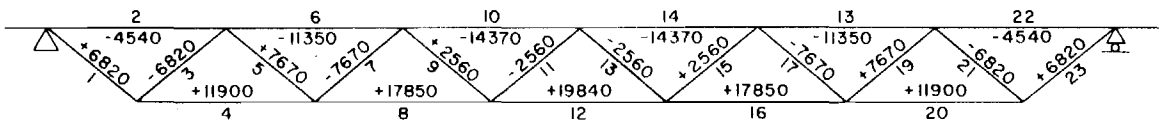

b) Stress Distribution in the Truss

(Stresses in lb/in^2; + = Tensile, - = Compressive)

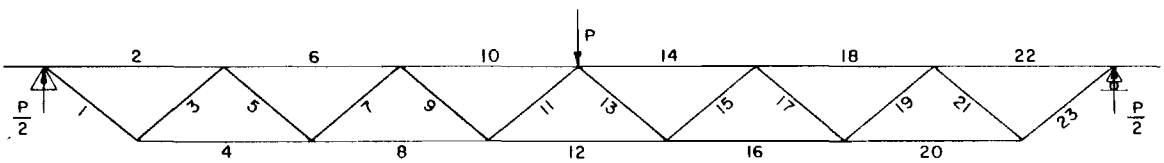

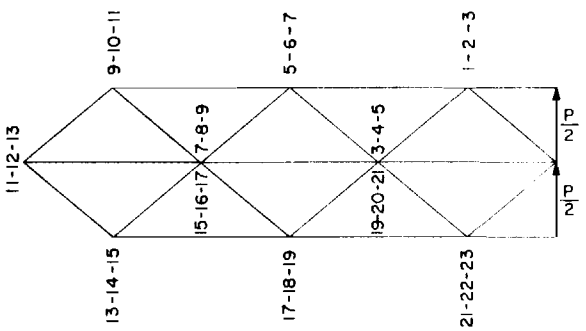

member m	S_{Pm}	$\frac{dS_{Pm}}{dP}$	member m	S_{Pm}	$\frac{dS_{Pm}}{dP}$
1, 23	$+1{\cdot}562\frac{P}{2}$	+0·781	7, 17	$-1{\cdot}562\frac{P}{2}$	-0·781
2, 22	$-1{\cdot}200\frac{P}{2}$	-0·600	8, 16	$+4{\cdot}300\frac{P}{2}$	+2·400
3, 21	$-1{\cdot}562\frac{P}{2}$	-0·781	9, 15	$+1{\cdot}562\frac{P}{2}$	+0·781
4, 20	$+2{\cdot}400\frac{P}{2}$	+1·200	10, 14	$-6{\cdot}000\frac{P}{2}$	-3·000
5, 19	$+1{\cdot}562\frac{P}{2}$	+0·781	11, 13	$-1{\cdot}562\frac{P}{2}$	-0·781
6, 18	$-3{\cdot}600\frac{P}{2}$	-1·800	12	$+7{\cdot}200\frac{P}{2}$	+3·600

c) Maxwell Diagram for a P Force on the Central Joint

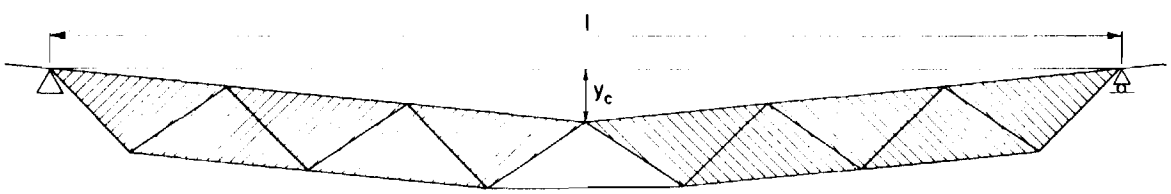

d) Simplied Model of the Truss

FIGURE 10
PROTECTED STEEL TRUSS USED AS EXAMPLE

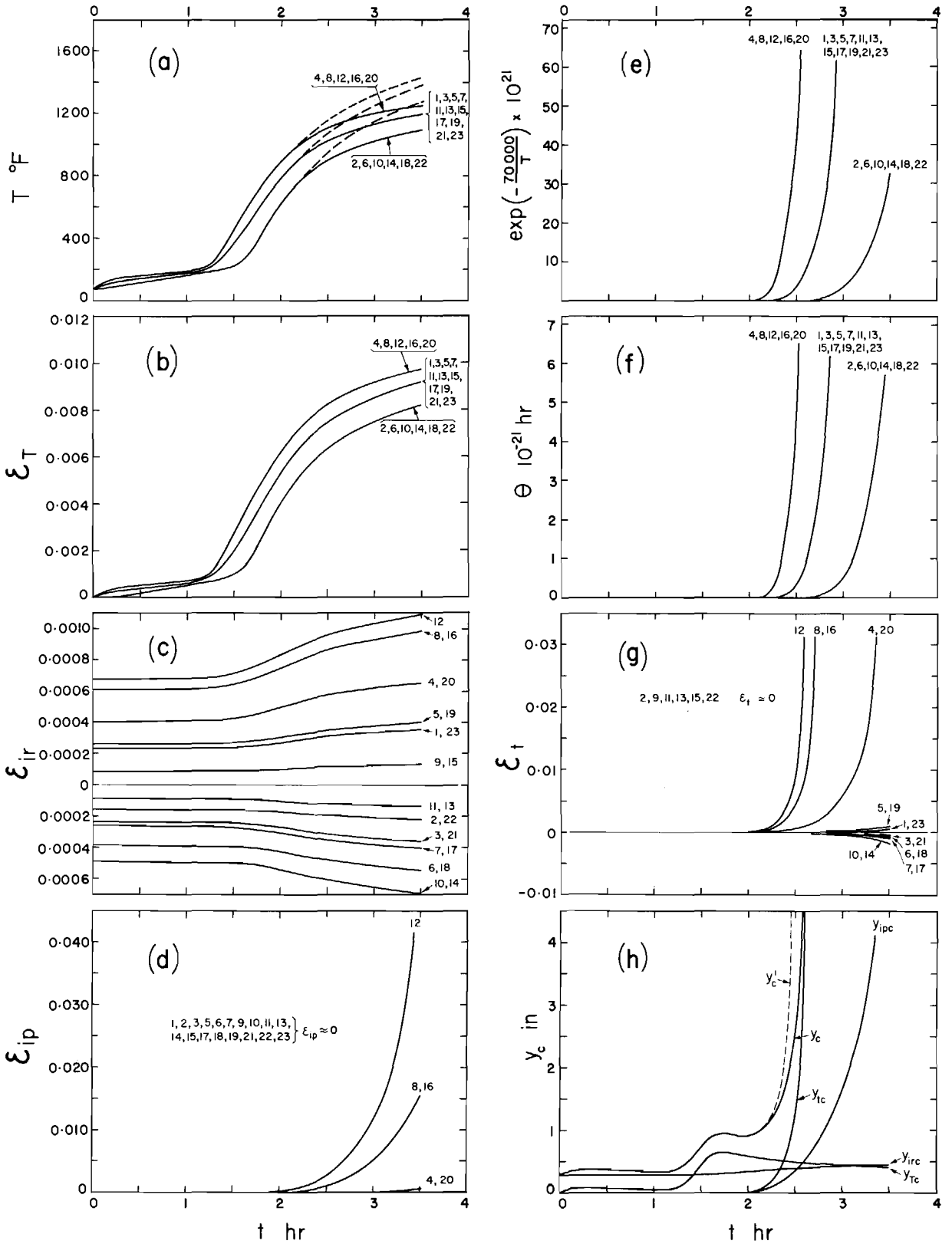

FIGURE II

CALCULATION OF CENTRAL DEFLECTION OF THE PROTECTED TRUSS SHOWN IN FIGURE 10a

(THE NUMBERS ON THE GRAPHS CORRESPOND TO THE NUMBERS OF THE TRUSS MEMBERS, AS SHOWN IN FIGURE 10)

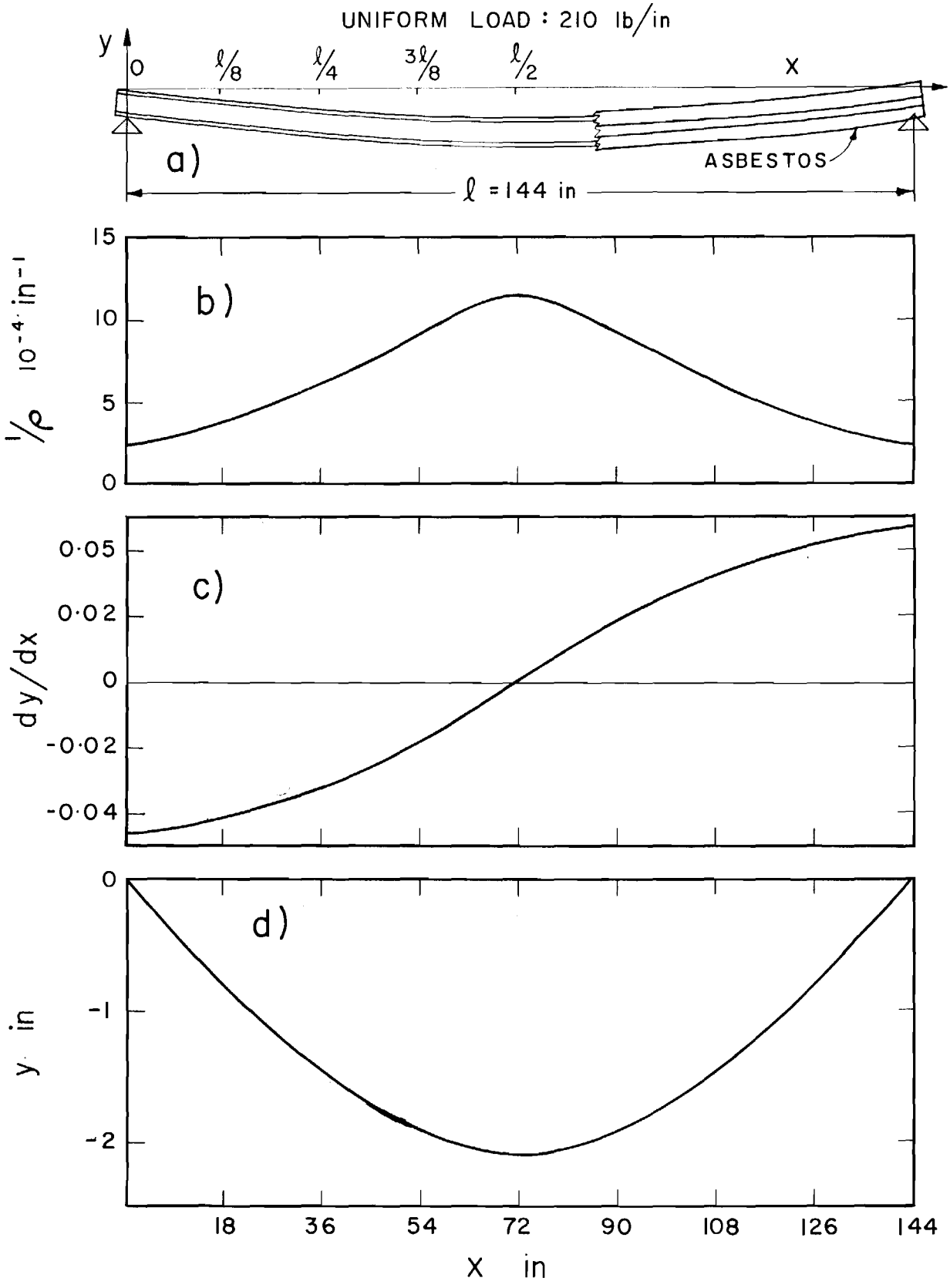

FIGURE 12

CALCULATION OF DEFLECTION OF A PROTECTED STEEL BEAM

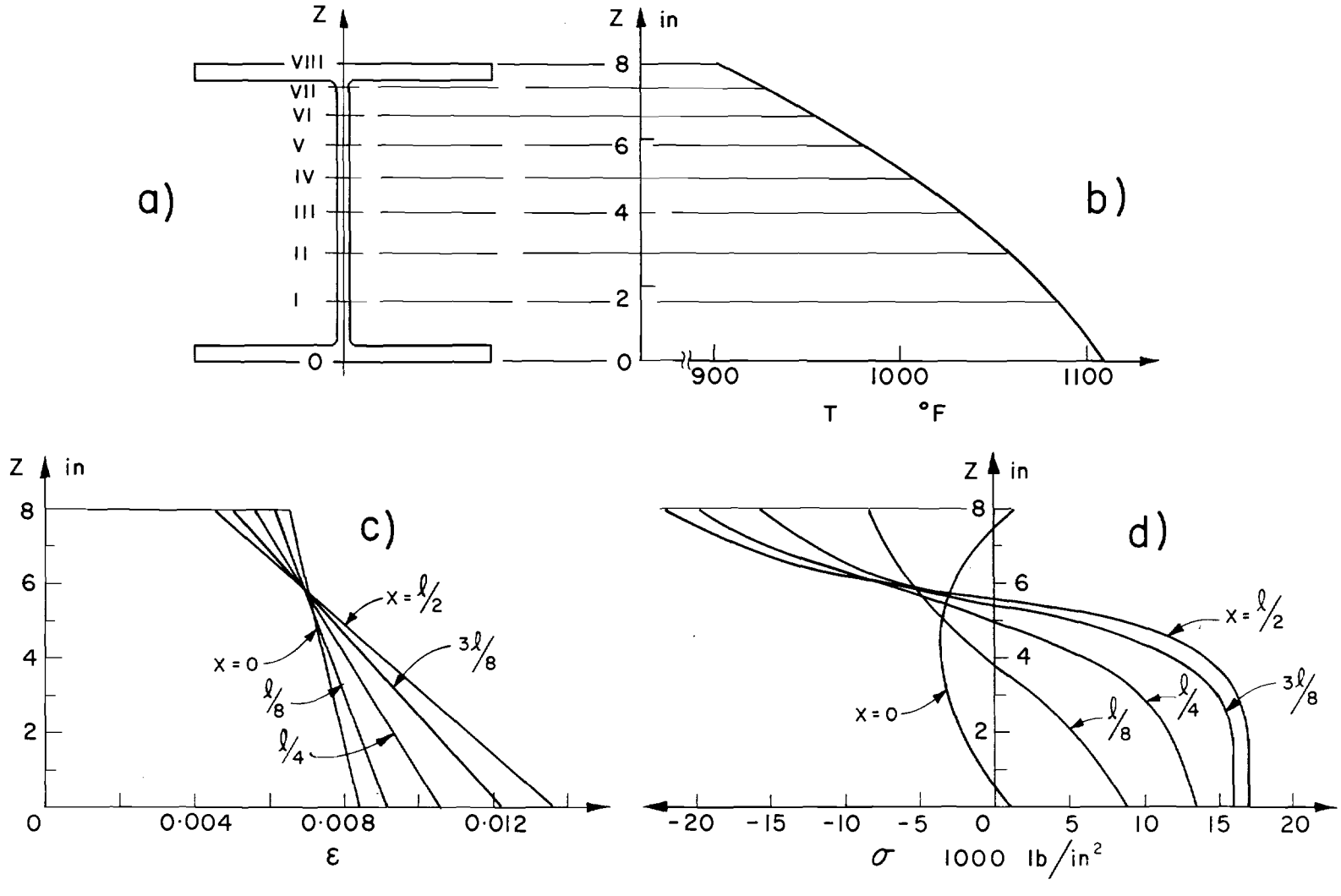

FIGURE 13

TEMPERATURE, STRAIN- AND STRESS DISTRIBUTION IN THE PROTECTED STEEL BEAM SHOWN IN FIGURE 12 a

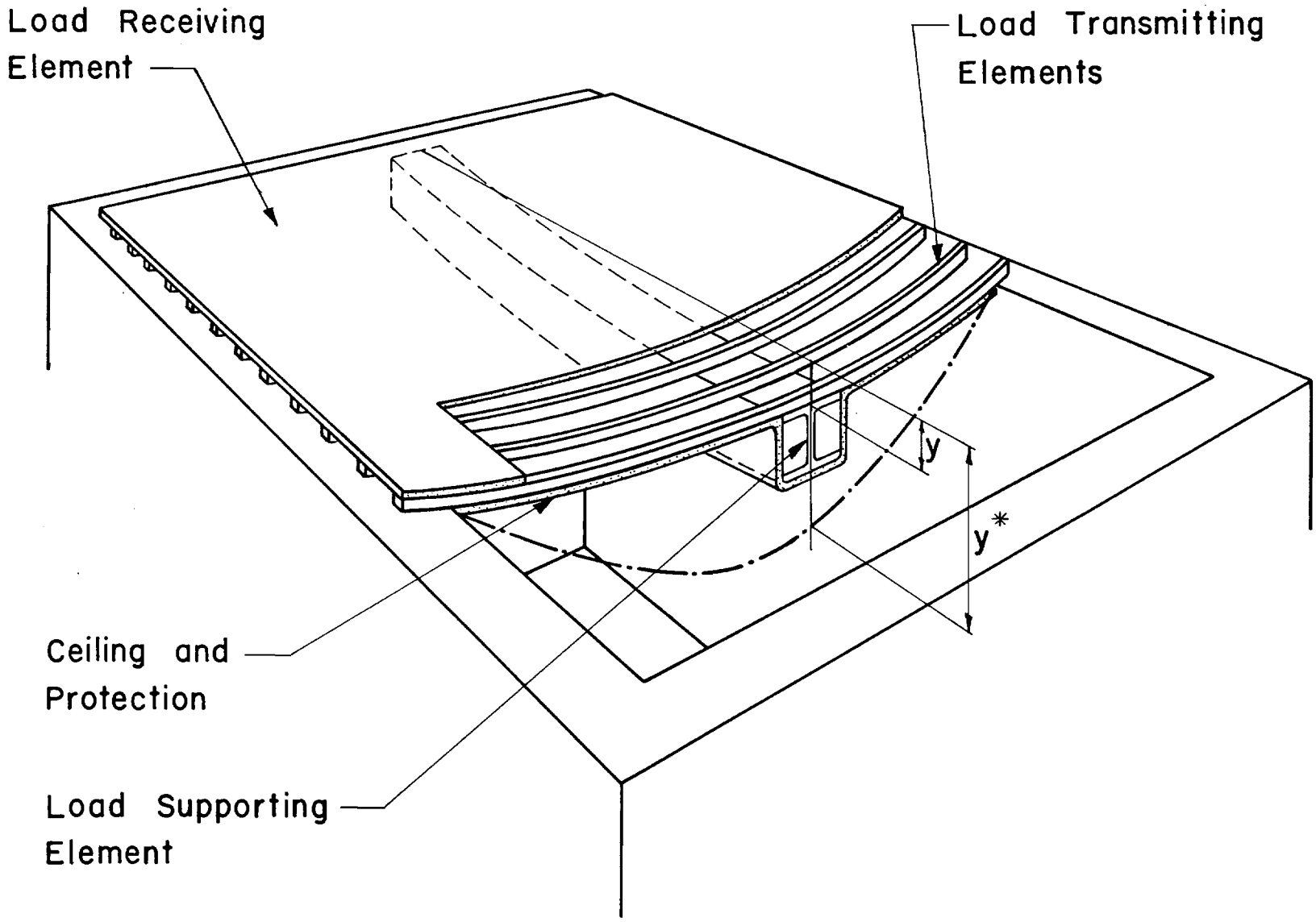

FIGURE 14

THE ELEMENTS OF AN ORDINARY FLOOR CONSTRUCTION

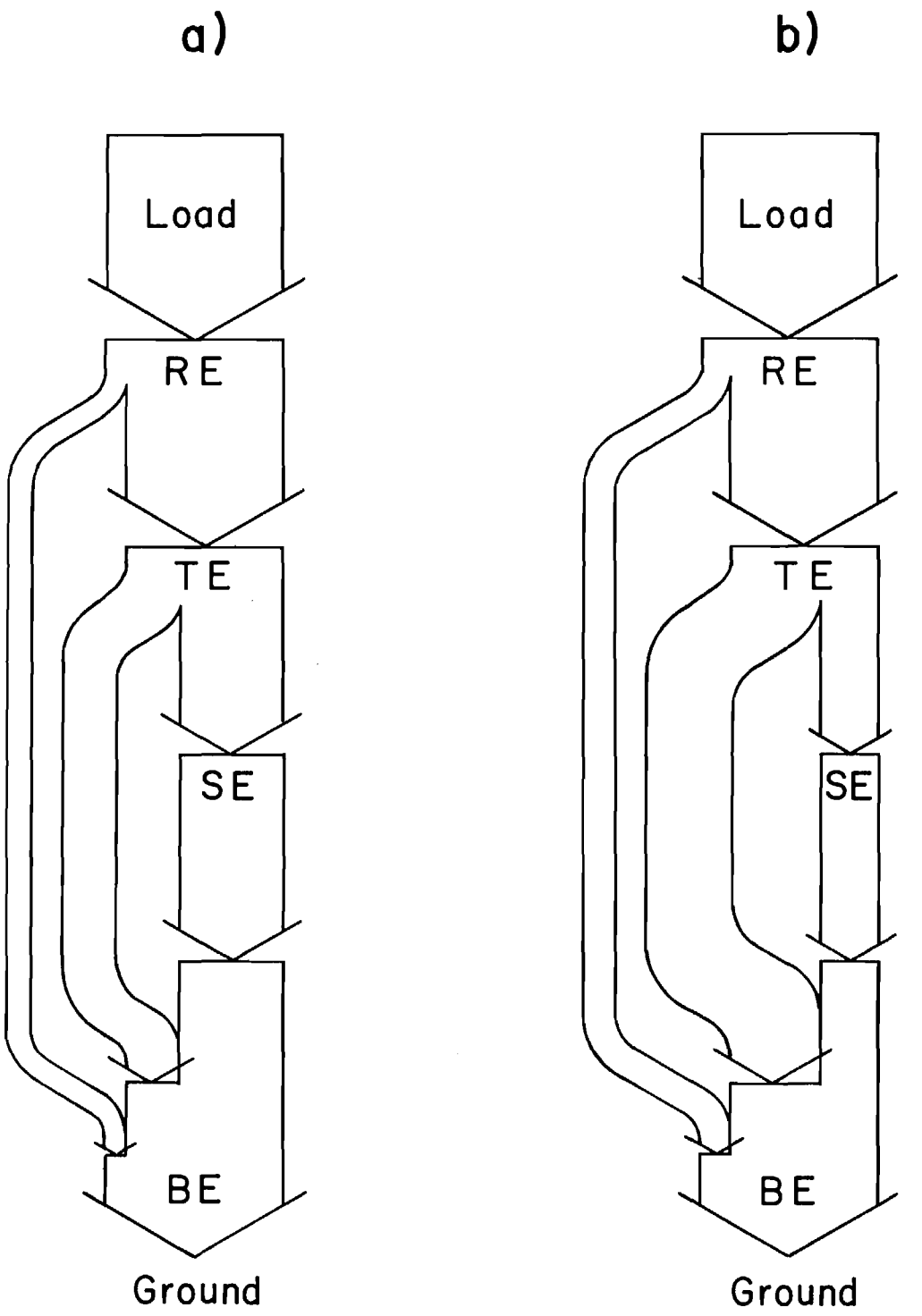

FIGURE 15 "LOAD FLOW" DIAGRAMS

a) BEFORE FIRE TEST

b) NEAR THE END OF FIRE TEST

RE = RECEIVING ELEMENT, TE = TRANSMITTING ELEMENT

SE = SUPPORTING ELEMENT, BE = BEARING ELEMENT

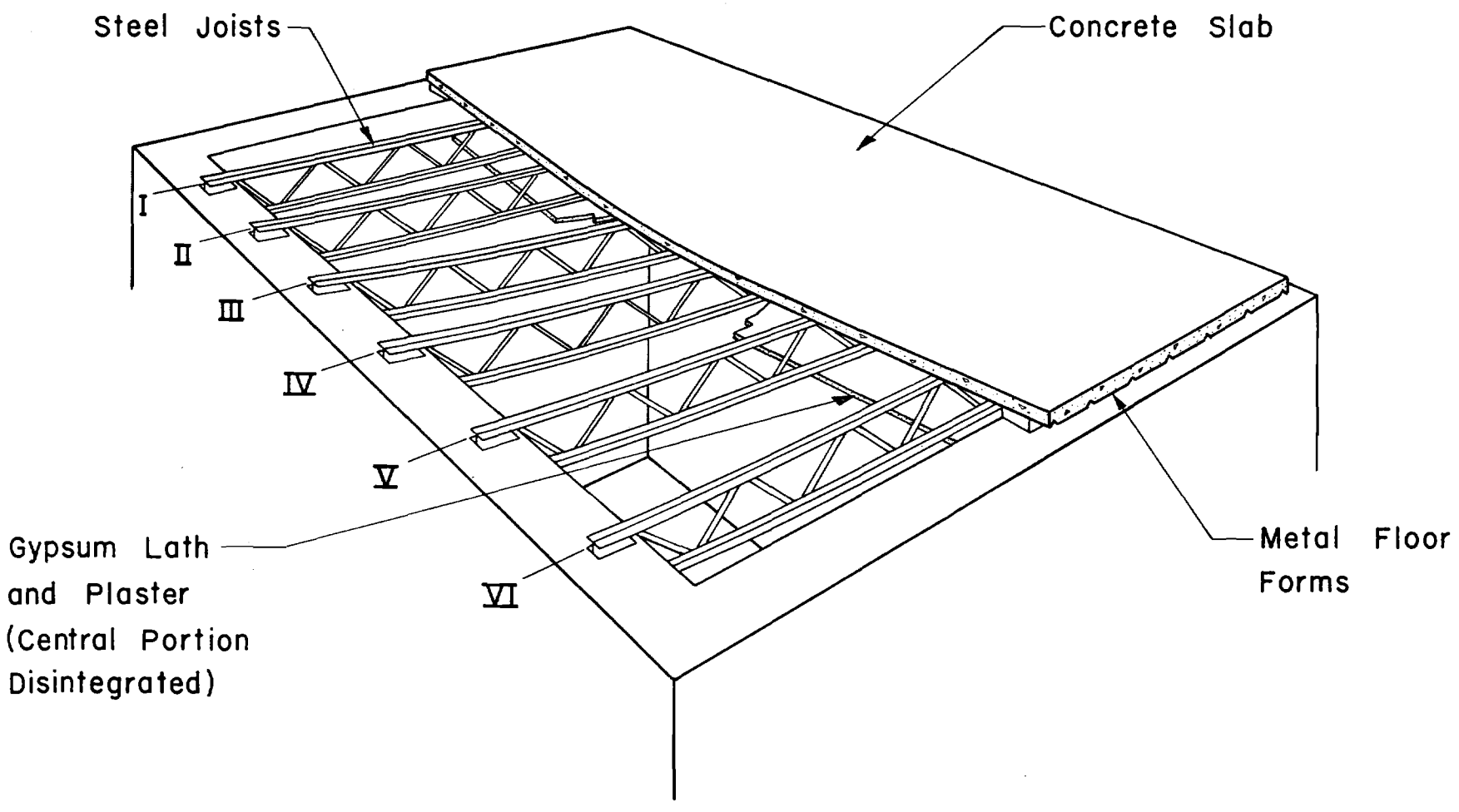

FIGURE 16

CONSTRUCTION WITH PARALLEL SUPPORTING ELEMENTS

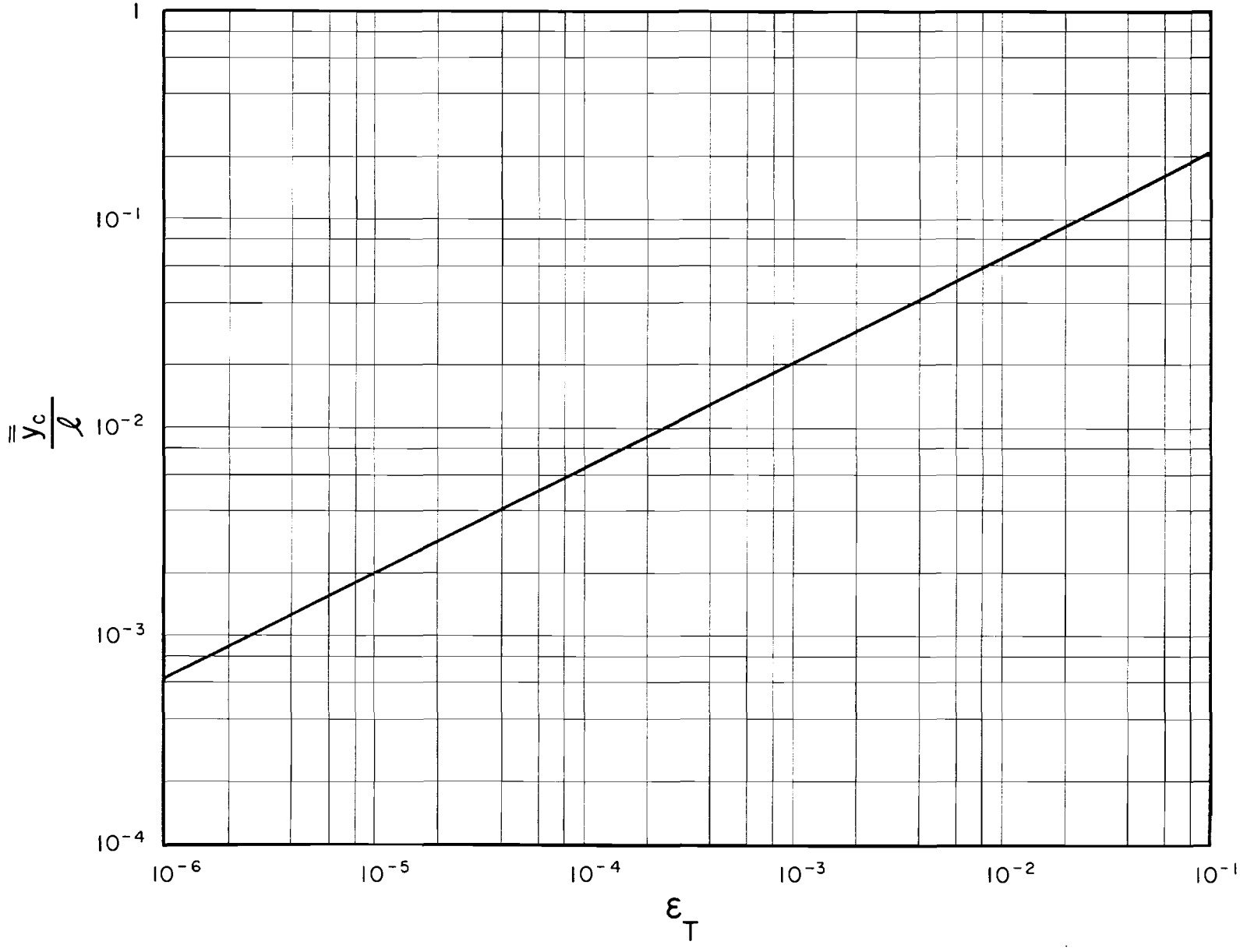

THERMAL DEFLECTION DUE TO EDGE RESTRAINT

FIGURE 17

BR 2275